Graduate Theses & Non-Theses   Student Scholarship

Spring 2019

USING GROUNDWATER MODELING TO ASSESS GROUNDWATER AND STREAM CONNECTIVITY IN A RIVER RESTORATION APPLICATION

John Joseph Lunzer

USING GROUNDWATER MODELING TO ASSESS GROUNDWATER AND STREAM CONNECTIVITY IN A RIVER RESTORATION APPLICATION

by

John Joseph Lunzer

A thesis submitted in partial fulfillment of the
requirements for the degree of

Masters of Geoscience in Hydrogeological Engineering

Montana Technological University

2019

Abstract

Historic placer mining operations along the Middle Fork John Day River (MFJD) north of Galena, Oregon have left the MFJD channel straightened, incised and lacking in riverbed structure. This lack of riverbed structure makes this stretch of the MFJD poor habitat for trout and migrating salmon. In order to restore this stretch of the MFJD to better serve aquatic species, Inter-Fluve Inc. (IF), United States Forest Service (USFS) and The Freshwater Trust (TFT) will be performing restoration to both the MFJD channel as well as Bear Creek, a tributary of the MFJD. The proposed restoration work will consist of re-routing of the MFJD and Bear Creek, re-meandering of the MFJD and construction of riverbed structure throughout the MFJD.

In preparation for this proposed restoration, the connectivity of groundwater and surface water throughout the reach must be assessed. The main focus of this groundwater and surface water connectivity assessment will be to characterize how wetlands located along the reach interact with surface water features via groundwater. Characterizing the connection between groundwater and surface water will aid in determining the potential risk of proposed restoration having negative impacts on wetlands located along the reach. In order to fully characterize the groundwater and surface water connectivity at the site, a monitoring plan focused on geologic, hydrogeologic and hydrologic characteristics was implemented. Data obtained from site monitoring was used to support a groundwater model for the site. This groundwater model was used to make predictions of how proposed restoration would impact the site wetlands.

Steady state and transient groundwater models of observed conditions calibrated relatively well producing low error values. Groundwater models revealed that initial restoration performed on Bear Creek has had a negative impact on the site wetlands. When all proposed restoration work is modeled, an overall increase in wetland water elevations is predicted throughout most the wetland area. Water elevations near the abandoned Bear Creek channel however, show a decrease in water elevation when all restoration work is implemented. This decrease in water elevation only occurs between May and July; modeling of July through October in this area show an increase in water elevation levels. Overall when all proposed restoration is completed, the site wetlands and entire site in general will benefit in terms of higher water elevations, especially during base flow conditions.

Dedication

I'd like to dedicate this thesis to those who have stubbornly and constantly kept faith in me as a person. There have been times I didn't even believe in myself on this journey and I have been blessed to be surrounded by the greatest support group on the planet. To quote the great Batman, "Sometimes people deserve to have their faith rewarded." This thesis is my reward to those who have shown faith in me as an individual, a friend, a brother, a son and a fellow passenger on this unforgettable journey we call life. None of this would be possible without my friends and family. Thank you all for everything.

I'd like to end this dedication with a quote from Jack Kerouac that I think accurately describes the people who shaped me into the person I am today.

"Here's to the crazy ones. The misfits, the rebels, the troublemakers. The round pegs in the square holes. The ones who see things differently. They're not fond of rules. And they have no respect for the status quo. You can quote them, disagree with them, disbelieve them, glorify or vilify them. About the only thing that you can't do, is ignore them because they change things. They invent. They imagine. They heal. They explore. They create. They inspire. They push the human race forward. Maybe they have to be crazy. Because the ones who are crazy enough to think that they can change the world, are the ones who do."

This work is also dedicated to my good friend, Chad Young. You'll always remain an inspiration to my life.

Acknowledgements

- Professor Glenn Shaw

- Committee members

    o Professor Larry Smith

    o Professor Robert Pal

    o Professor Raja Nagisetty

    o Professor Liping Jiang

- Andy Bobst, MBMG

- Donna Conrad

- Nick Barney

- Jeffrey & Cathy Lunzer

- Gardner Johnston

- Matt Cox

- Pollyanna Lind

- The Freshwater Trust

- United States Forest Service

Table of Contents

List of Tables

List of Figures

List of Equations

1. Project Overview

1.1. Purpose

River restoration has become a rapidly growing industry and field of science. Generally the focus of river restoration efforts is on restoring channel structure by altering sinuosity, riffle-pool sequences, spawning habitat, secondary channels and vegetation. These efforts usually consider hydrologic parameters such as design flow rate, flood frequency and connectivity to floodplain [Groot et al., 2008]. Typically river restoration projects have not had a focus on groundwater monitoring or modeling.

Currently groundwater – surface water interactions are often investigated with groundwater modeling techniques in situations where aquifer withdrawal begins to inhibit stream base flows. The complexity of these groundwater – surface water systems often requires the need for detailed monitoring of both groundwater and surface water features [Baird et al., 2005, Fleckenstein et al., 2014]. These studies are often larger scale and seek to predict long terms impacts to an aquifer system.

Hyporheic exchange is also an area of relatively intense study in regards to characterizing groundwater – surface water interactions. These studies are typically small scale with a focus on understanding how river restoration efforts serve to increase hyporheic exchange in a system. These studies can range from groundwater models of restored systems to theoretical models quantifying the increase in hyporheic exchange based off increasing channel sinuosity [Kasahara & Hill, 2008, Boano et al., 2006].

In the past ten years information on baseline conditions and monitoring after most river restoration work has slowly begun to draw more scientific interest. By monitoring and studying groundwater –surface water interaction before and after systems are restored, the ability to create

efficient and effective, science based restoration design plans will improve. Monitoring and modeling river systems before they are restored will allow for the ability to make predictions of long-term effects of proposed restoration work. This in turn will directly aid in the prevention of unforeseen or unintended consequences from restoration efforts. [Schneider et al., 2011, Rogiers et al., 2011].

Typically baseline conditions surveys and restoration monitoring studies do not investigate groundwater on a detailed scale and even fewer use monitoring efforts to support groundwater models. The potential usefulness of groundwater models in river restoration is abundantly apparent and a major proponent of the objectives of this project. The main objectives of this thesis project are to; i) implement a pre-restoration monitoring plan for a site that is going to be restored with common river restoration techniques, ii) use collected monitoring data and a field site investigation study to produce a groundwater model, iii) use the constructed groundwater model to make predictions of how proposed restoration work will impact groundwater – surface water interactions at the site, iv) use the model results to provide practical, sound recommendations to directly aid the proposed restoration design.

1.2.   Site description

The Middle Fork John Day River (MFJD) is located in east-central Oregon near the town of Galena in Figure 1. Historic placer mining in the region has left sections of the MFJD channelized and surrounded by piles of remnant mine waste rock. In this channelized state, the MFJD has limited floodplain connection and provides little spawning habitat for salmon and trout species. One such mining impacted section of the MFJD located 2.0 miles north of Galena, known as the Galena Tailings Site (GTS), is currently in the design process for restoration (Figure 1). This restoration will be performed through a collaborative effort between Inter-Fluve,

Inc. (IFI), the United States Forest Service (USFS) and The Freshwater Trust (TFT). Restoration

plans aim to re-meander and reconnect the MFJD to its floodplain and reconnect nearby tributary
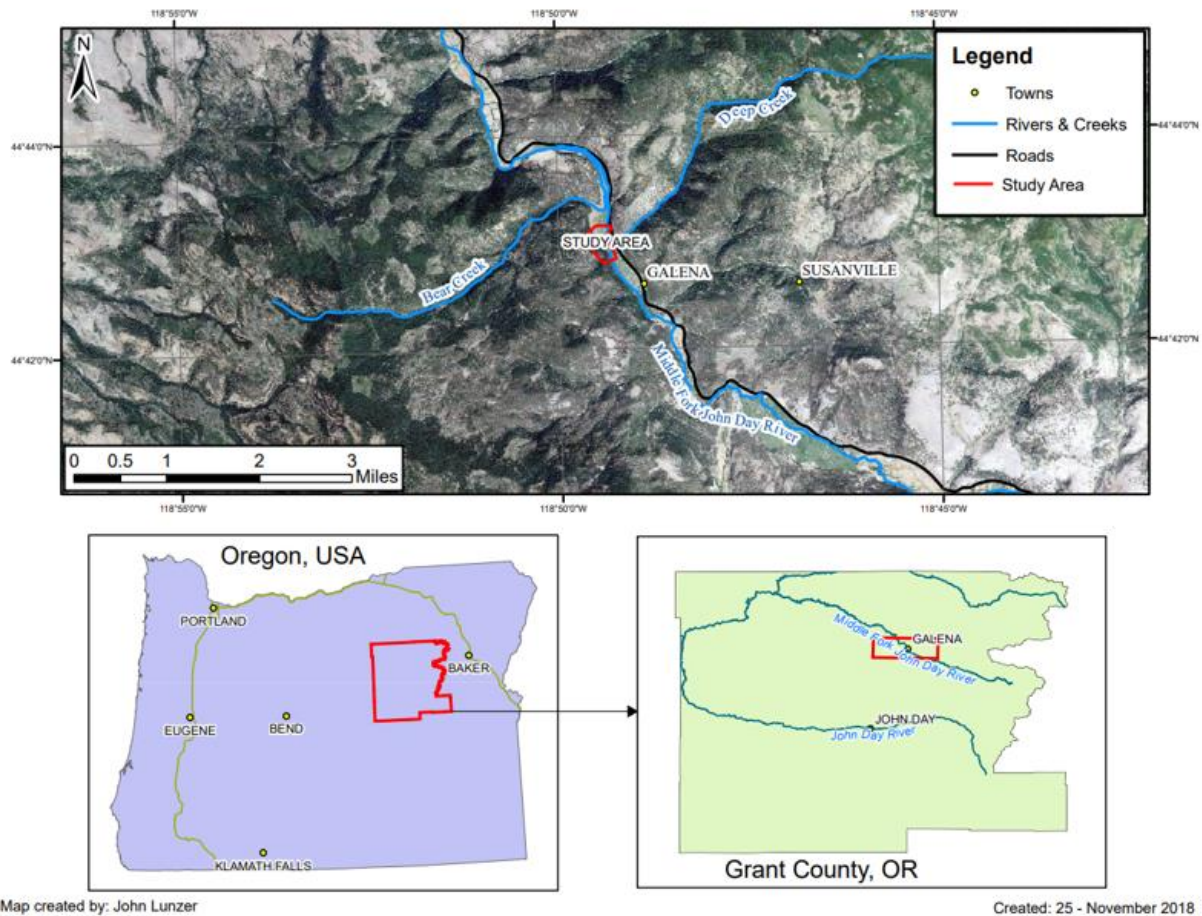
Bear Creek to the MFJD. Existing wetlands at the GTS are primarily fed by a channel of Bear

Creek; this channel will be removed as per current restoration plans.

Figure 1: Inset maps showing the location of the Galena Tailings Site (GTS). Imagery and data from Oregon.gov.

1.3. Modeling objectives

The proposed restoration plans pose a potential risk to the long-term health of the GTS

wetlands. Both the re-meandering of the MFJD as well as the removal of the Bear Creek channel

that feeds the wetlands will change hydrologic stresses on the wetlands. Current site conditions,

proposed-restoration conditions and detailed Bear Creek proposed-restoration conditions are

depicted in Figures 2, 3 and 4 respectively. In order to determine the net impacts of proposed

restoration on the GTS wetlands, a groundwater study was performed in order to produce a

groundwater flow model of the GTS under pre- and post-restoration conditions. Groundwater

modeling was supported by a field monitoring program. Pre- and post-restoration conditions

were modeled and recommendations were made for a restoration plan that meets all MFJD

restoration goals while maintaining the health of the wetland area.
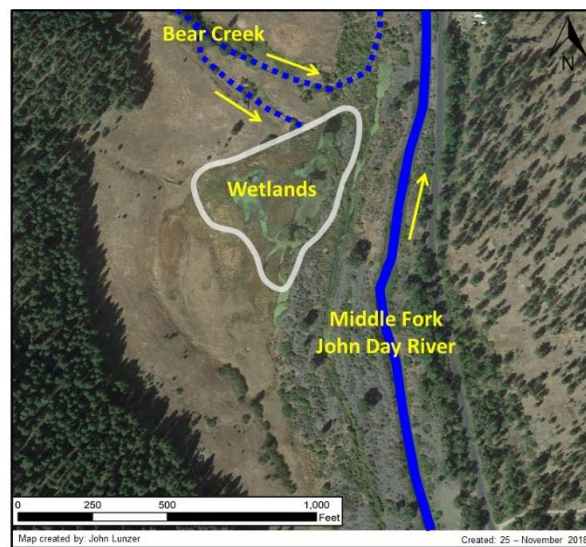
Figure 2: Current site conditions map depicting Middle Fork John Day River (solid, blue), Bear Creek channels (dotted, blue) and wetlands extent (solid, white). Yellow arrows indicate flow direction of surface water features. Imagery from GoogleEarth.
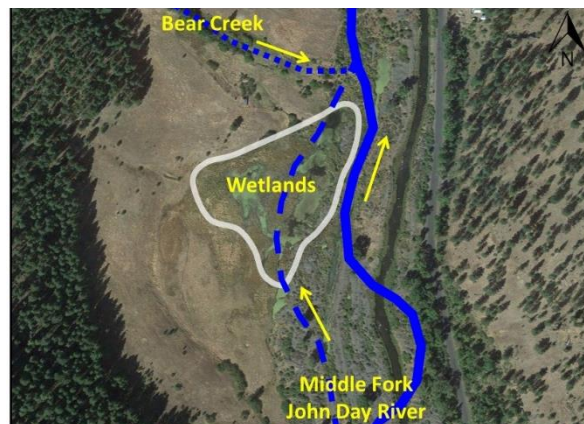
Figure 3: Simplified post-restoration conditions map depicting Middle Fork John Day River main channel (solid, blue), Middle Fork John Day River secondary channel (dashed, blue), Bear Creek channel (dotted, blue) and wetlands extent (solid, white). Yellow arrows indicate flow direction of surface water features. Not all secondary channels are shown. Imagery from GoogleEarth.
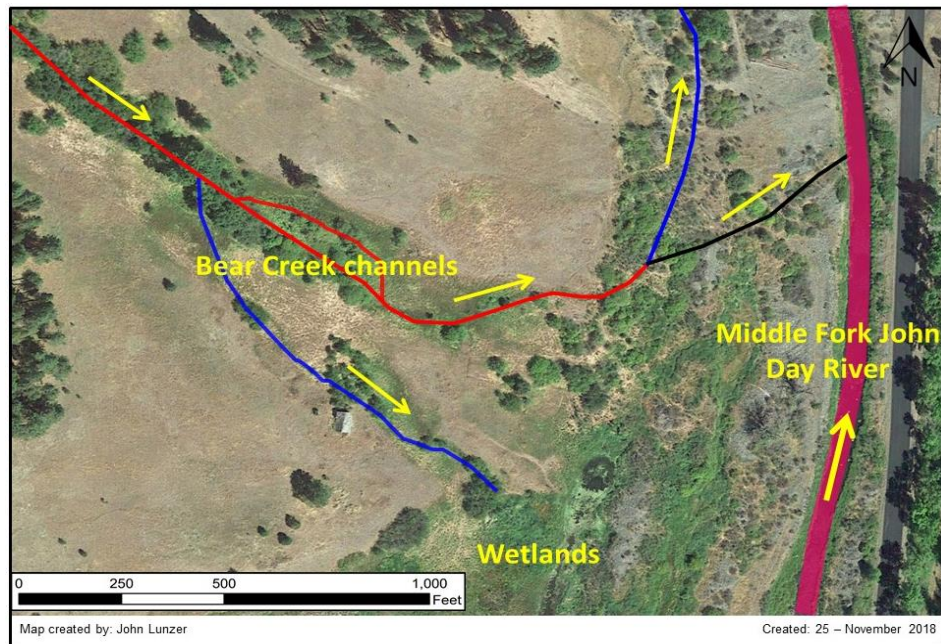
Figure 4: Simplified Bear Creek post-restoration conditions map depicting Bear Creek existing channels to remain (red), Bear Creek channels to be removed (blue), Bear Creek channels to be constructed (black) and the Middle Fork John Day River (pink). Yellow arrows indicate the flow direction of surface water features. Imagery from GoogleEarth.

2. Site Background and Conditions

2.1. History

Mining operations have taken place in the MFJD watershed, formally known as the Susanville mining district, since placer mining began along Elk Creek in 1864 [Lindgren, 1901]. Significant placer mining operations continued until the 1950s when most operations were abandoned. These placer mining operations moved large amounts of waste rock through dredges, sluices and other pieces of mining equipment [Dept. of Geology & Mineral Industries, 1957]. Additionally mining operations channelized the MFJD in several reaches as well as channelized many of the main tributaries to the MFJD. At the GTS, placer mining operations channelized the MFJD and left large piles of mine waste rock directly west of the MFJD. These piles of mine waste rock stretch the entire length of the site from south to north along the MFJD. This mine waste rock consists predominantly of coarse sand, cobbles and boulders with metal scraps throughout. The GTS is currently owned and managed by the USFS as public land used for recreation, grazing and logging.

2.2. Topography

Topography at the GTS consists of valley and mountain terrain between 3375 ft and 3450 ft above sea level. The majority of the site lies within a relatively flat mountain valley that experiences a drop of roughly 15 ft across the GTS. The west boundary of the GTS is made up of mountain terrain that is significantly steeper than the rest of the terrain at the GTS. The northwest boundary of the GTS is an alluvial fan. This terrain is not as steep as the mountain terrain to the west but is significantly steeper than the valley terrain.

Light detection and ranging data (LiDAR) were available for the site from the State of Oregon Department of Geology and Mineral Industries [Dept. of Geology & Mineral Industries,

2010]. This LiDAR survey was shot in August 2010 with roughly 30 returns per square meter

providing high resolution data (Appendix A-1). Additionally the LiDAR data were available in

formats that showed both bare ground surface and vegetation at the site.

2.3. Geology

2.3.1. Surficial

Site geology was characterized using the United States Geological Survey (USGS)

produced *Geologic map of the Canyon City quadrangle, northeastern Oregon* [Brown & Thayer,

1966]. The site scale geology can generally be described as Mesozoic metasedimentary and

volcanic rocks. These units typically are present as subsurface bedrock and surface exposures

throughout the region. At the site, these Mesozoic rocks are typically basalts that are overlaid by

Quaternary alluvium deposits that consist of sands, gravels and cobbles. Figure 5 shows the

USGS geologic map with site boundary marked.
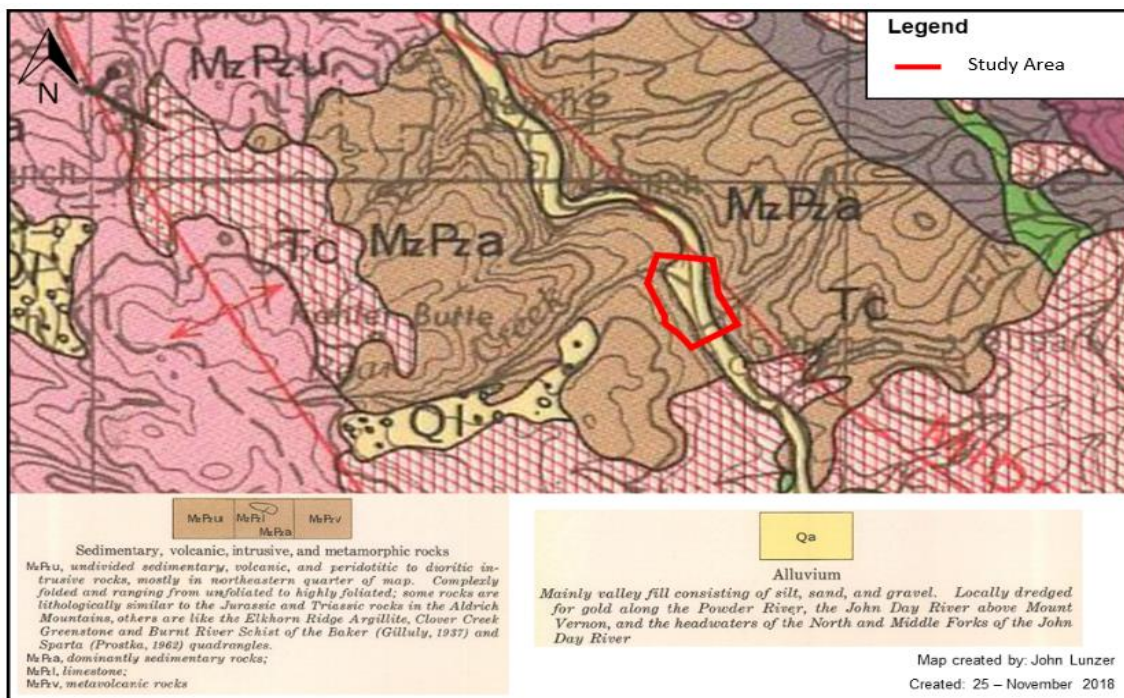
Figure 5: Geologic map with the study area outlined in red. Study area is underlain by volcanic and sedimentary rock. Quaternary alluvium sediments make up the study area surficial deposits. *Geologic map of the Canyon City quadrangle, northeastern Oregon* [Brown & Thayer, 1966].

2.3.2. Subsurface

Data describing subsurface conditions are available through the Oregon Water Resources
Department Well Report Query [Oregon Water Resources Dept., 2019]. In total nine public well
records were available within 4.0 miles of the site (Appendix A-2). Pertinent information from
these well records included distance from the GTS, well depth, depth to bedrock and whether the
well was located in the valley or on the mountain front (Table I). The four wells located 0.75
miles south of the GTS in the valley sediments revealed bedrock to be between 22.0 feet (ft) and
42.0 ft below ground surface (bgs).

Table I: Summary of subsurface conditions from publicly available well logs

Well ID	Approximate distance from site (miles)	Well depth (ft)	Well location	Depth to bedrock (ft)
GRAN_51292	0.75	106.0	Valley	22.0
GRAN_50256	0.75	87.0	Valley	35.0
GRAN_50052	0.75	150.0	Valley	29.0
GRAN_50965	0.75	96.0	Valley	42.0
GRAN_51307	4.00	122.0	Mountain front	36.0
GRAN_50572	3.25	180.0	Mountain front	45.0
GRAN_50730	2.75	117.0	Mountain front	38.0
GRAN_50924	2.50	100.0	Mountain front	60.0
GRAN_51024	3.50	200.0	Mountain front	45.0

2.3.3. Aquifer

Based off surficial, subsurface and observed geologic data, the GTS aquifer is made up of
two distinct materials. The valley aquifer material itself is relatively coarse sands, gravels and
cobbles ranging from 22.0 ft to 42.0 ft thick. The material making up the second major aquifer
unit at the GTS is the finer alluvial fan sediment which is predominantly sands, silts and clays.
The majority of the GTS is made up of the coarser valley aquifer sediment while the alluvial fan
sediment makes up only the northwest portion of the GTS. The location of these two aquifer
materials is determined based off the location of the alluvial fan. The coarse valley aquifer in

places is overlaid with a thin 0.5 ft to 5.0 ft layer that consists predominantly of silt and clay. This unit is typically present in the wetland region and is overall discontinuous throughout the site.

2.1. Surface water flows

Discharge data for the MFJD was obtained from the USGS National Water Information System, USGS 14043840 [USGS, 2019]. The gage station producing this data is located 3.15 river miles upstream of the GTS and is located at the confluence of the MFJD and Camp Creek. This station records MFJD stage and discharge every 15 minutes. The station also records river temperature every 15 minutes. The MFJD experiences flow rates between 10.0 cubic feet per second (cfs) and 1000.0 cfs depending on the time of year.

2.2. Watershed area

The entire MFJD watershed is roughly 507,000 acres in area and terminates were the MFJD joins the North Fork John Day River. The watershed area contributing to the MFJD upstream of the GTS is roughly 275,000 acres. The Bear Creek watershed area is roughly 11,000 acres; approximately 4.0% the size of the MFJD watershed area contributing to the MFJD flow at the GTS [Oregon BLM, 2019].

2.3. Climate

The climate conditions of the GTS can be generally characterized as similar to the nearby town of John Day, Oregon. During the period of May 2018 through September 2018, the area received slightly less precipitation than normal and experienced slightly colder temperatures. The exception to this is October 2018 which experienced more precipitation than normal. Typically the period of May through October experiences around 5.12 inches (in) of total precipitation, however May 2018 through October 2018 experienced 4.09 in of total precipitation. Table II

displays a summary of average and 2018 precipitation totals for the John Day area [U.S. Climate Data, 2018]

Table II: Site precipitation levels for 2018 and average years.

Month	Average Precipitation (in)	2018 Precipitation (in)
May	1.80	1.62
June	1.40	1.01
July	0.51	0.10
August	0.72	0.08
September	0.70	0.04
October	1.01	1.24

3. Methods

3.1. Groundwater monitoring

In order to monitor groundwater conditions at the site, monitoring wells and staff gauges were installed throughout the entire GTS. Monitoring wells were placed in the open valley grasslands to the southwest of the wetlands as well as east of Bear Creek. Staff gauges were placed throughout the tailings ponds and wetlands, which were considered groundwater ponds. Figure 6 shows the location of all installed monitoring equipment. All monitoring equipment was surveyed by IFI using pre-surveyed rebar and control points. Surveying was performed with a Topcon GR-5 base and rover system.

Figure 6: Monitoring equipment locations. Monitoring wells (MW) marked in yellow, staff gauges (SG) marked in red.

3.1.1. Monitoring Wells

Figure 7: Hand cutting well screen slots with a hacksaw

Monitoring wells were constructed by first excavating a boring using post hole diggers and a 2.0 inch diameter bucket auger. During excavation of the boring, subsurface lithology was recorded and in several borings soil samples were taken. Boring continued until auger refusal was met which typically occurred between two ft and five ft bgs on coarse gravel and cobbles. Once the boring was constructed a 1.0 inch diameter PVC pipe was inserted into the boring. The bottom 18 in of each well pipe was slotted every 0.25 inches using a hacksaw and the bottom end of the pipe was capped (Figure 7). Once the well pipe was lowered into the boring, engineered well pack sand was poured into the boring, around the well pipe until the bottom 24 inches of the

Figure 8: Monitoring well installed at GTS

boring was filled with sand. This ensures that the entire well screen is surrounded by sand pack. Next bentonite clay chips were poured into the boring around the well pipe. Bentonite was added until the boring was filled nearly to the surface. This ensures no surface water enters the boring and well. A well construction and geologic log were created for each well and can be found in Appendix B-1. Once the well pipe was placed and the boring was filled properly, each well pipe was cut off roughly three ft above the ground surface, labeled and capped (Figure 8). Nine totals monitoring wells were installed at the site between May 10, 2018 and June 23, 2018.

Water levels in monitoring wells were manually measured twelve times between May 10, 2018 and October 13, 2018. Manual measurements were taken in each monitoring well using a

Slope Indicator Company – Water Level Indicator. Marks were placed on the rim of each well pipe to ensure that the water levels were measured from the same side of the well pipe each time. In addition to manual measurements, Solinst Levelogger Edge pressure transducers were placed in several monitoring wells between July 14, 2018 and October 13, 2018. A separate barometric pressure transducer was placed in open air at the site to allow each transducer data set to be corrected for changes in barometric pressure.

3.1.2. Staff Gauges

Staff gauges used at the GTS consisted of 1.5 inch by 0.5 inch by 36.0 inch wood slats. These slats were hand painted with alternating white strips marking every tenth of a foot along the slat. Metal cattle fence posts were then pounded into the pond bottom with a fence post pounder. Once the fence posts were pounded into the pond bottom, the painted wood slats were attached firmly to the fence post with multiple zip ties and labeled (Figure 9). Twelve staff gauges were installed at the site between May 26, 2018 and June 22, 2018. Distance from the top of the staff gauge to the water surface was recorded visually twelve times between May 26, 2018 and October 13, 2018. Additionally, Solinst Levelogger Edge pressure transducers recording water levels every 15 minutes were placed at the bottom of SG6 and SG9 between August 10, 2018 and October 13, 2018 using fishing

Figure 9: Staff gauge installed in a tailings pond at the GTS

line and zip ties. A separate barometric pressure transducer was placed in open air at the site to

allow each transducer data set to be corrected for changes in barometric pressure.

3.1.3. Temperature and Specific Conductivity

In addition to water level measurements,

temperature and specific conductivity were

measured in each monitoring well and each

tailings pond. These measurements were taken

using a Hand-held pH/Cond Mutli 340i probe.

For monitoring wells the probe was inserted into

Figure 10: Multi 340i probe measuring temperature and specific conductivity in a monitoring well

each well and left until the temperature stabilized at which point temperature and specific

conductivity were recorded (Figure 10). For staff gauges, the probe was placed at a depth in the

middle of the pond water column immediately next to the staff gauge. The probe was left in the

pond until temperature stabilized at which point temperature and specific conductivity were

recorded.

3.2. Surface water monitoring

3.2.1. Middle Fork John Day River

In addition to discharge and stage data for the MFJD provided by the USGS gauge station

discussed in Section 2.4, two sets of manually measured stage and discharge were taken at the

GTS. Manual measurements were taken to confirm that the discharge on MFJD at the GTS was

the same as the discharge measured at the upstream USGS gauge station. Additionally this

manual measurement was made to determine the stage based on discharge at the GTS. Manual

discharge and stage measurements were made on the MFJD at the GTS using a Marsh-McBirney

flow meter and the velocity-area discharge calculation method [Fetter, 2014]. Two complete

cross sections of the channel were measured on December 12, 2018. These cross sections were compared with USGS gauge data to determine stage in the MFJD at the GTS based off discharge.

3.2.2. Bear Creek

Bear Creek discharge was measured in all flowing channels during each site visit. Before restoration, Bear Creek consisted of five separate channels named A, B, C, D and E (Figure 11). After restoration, Bear Creek consists of four separate channels named A, C, D and F also seen in Figure 11. Each site visit, discharge was measured in all channels with measureable flow. Typically flow measurements were taken with the salt slug tracer method [Winter, 2014, Day, 1976, Hongue, 1987]. This technique involved using rhodamine dye to first determine with a given injection point in the channel at what point downstream complete mixing occurs. This
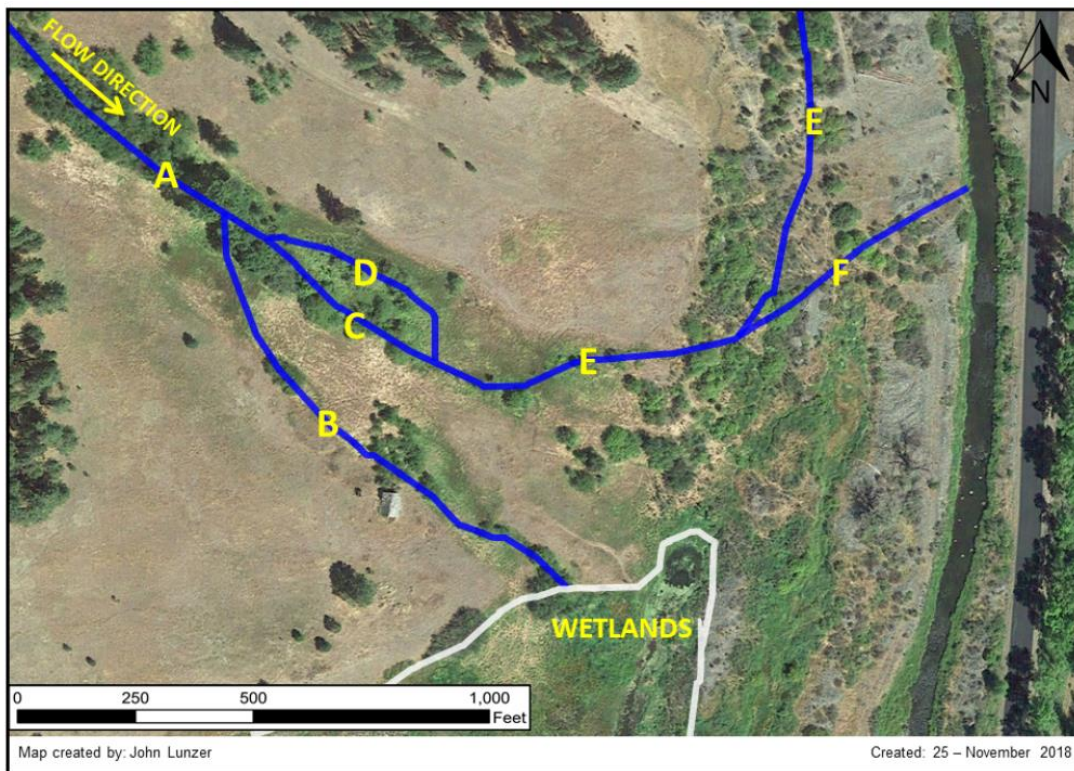
point is made apparent as the point in which the entire stream channel is uniformly pink from the

Figure 11: Map depicting the location of all Bear Creek channels

dye. Once this point was determined, a Mutli 340i probe was placed at the point of complete mixing and background specific conductivity and temperature were recorded. After recording background channel conditions, a 100 mL salt slug with 12.5 g of dissolved salt was injected upstream of the Mutli 340i probe. Upon injection of the slug, specific conductivity measurements were taken from the Mutli 340i probe downstream. These specific conductivity measurements were typically taken every 2 seconds until the conductivity in the stream returned to background levels indicating the entire salt slug had passed through the stream. This process was repeated three times in each channel to produce a range of discharges for that particular channel and day. Time since injection and conductivity levels were input into a Montana Technological University owned Microsoft Excel spreadsheet, which converted the input data into discharge in cubic feet per second.

All salt slugs were created by weighing 125.5 g of NaCl and mixing the NaCl in 1000 mL of deionized water using an Erlenmeyer flask. Once the NaCl was completely dissolved in the deionized water, the solution was split into ten 100 mL slugs using a 250 mL beaker and glass funnel. All slugs were placed in 125 mL HDPE plastic sample bottles, capped and labeled with their contents.

On one such occasion, channel flow was too low to use the salt slug tracer method. Instead the velocity area method was used to estimate discharge for this channel [Fetter, 2014]. Channel area was estimated using a tape measure to record the width and depth of the channel for one reach. After measuring channel area, a leaf was placed in this reach and the time for this leaf to travel 1.0ft and 2.0ft was recorded to determine channel velocity.

In total discharge measurements were made on all flowing channels of Bear Creek eight times between April 21, 2018 and October 13, 2018.

3.3. Hydraulic conductivity

3.3.1. Slug tests

To determine hydraulic conductivity of the discontinuous silt and clay sediment and the alluvial fan sediment, slug tests were performed in several of the monitoring wells screened in these sediments. Solinst Levelogger Edge pressure transducers were placed in the bottom of the well and set to record water levels every second. Once the transducers were placed in the well, they were allowed to sit for at least one hour to ensure water levels returned to static levels before the addition of the slug. Since the monitoring wells were 1.0 inch diameter PVC pipe, conventional cylindrical slugs could not be used to raise water levels. Instead approximately 240 mL of water was poured into each well, raising water levels roughly 18 inches. After adding the water slug to the well, the well was left for at least two hours to ensure water levels returned to static conditions before removing the transducer. Once the data was retrieved from the transducers, the slug test was input into the computer program *AQTESOLV* and analyzed using the Hvorslev method [Fetter, 2014]. Analysis was performed on each slug test for both a high and low estimates of hydraulic conductivity with the Hvorslev method.

In total eight separate slug tests were performed on MW1, MW3, MW8 and MW9 on 7/14/2018 and 7/21/2018.

3.3.2. Soil sieve analysis

To estimate hydraulic conductivity of the coarse sand, gravel and cobble aquifer, soil samples were collected and analyzed using a soil sieve analysis. Slug tests could not be used to determine hydraulic conductivity due to the fact that no monitoring wells were screened completely in the aquifer. Soil samples were collected near MW6 using a two-foot deep soil pit dug with a shovel. Soil samples were taken to Montana Technological University where sieve

analyses were performed on each sample in accordance with

ASTM Standard D6913, seen in Figure 12 [ASTM D6913].

Once the sieve analyses were performed, the particle size

distribution curves were used to determine the D_{10} particle size

for each sample. The D_{10} particle size is the particle size in

which 10% of the sample by mass is finer than. These D_{10}

particle sizes were used with a modified Hazen's Equation to

estimate hydraulic conductivity (Equation 1). Constant C was

found in literature to be 0.0 to 1.5 seen in Equation 1 [Svensson,

2014, Uma et al., 1989].

Figure 12: Soil sieves setup in accordance with ASTM D6913.

Equation 1: Modified Hazen's equation

$$K = C(d_{10})^2$$

Where:
K = hydraulic conductivity (cm/sec)
C = constant (typically 0.0 - 6.0)
d_{10} = particle size that 10% of sample is finer than by weight (mm)

3.4. Silt/clay layer thickness

To determine the thickness of silt and clay layer throughout the GTS a 0.375 inch

diameter, 5.0 ft-long steel rod was used to probe the soil. This probing was performed every 20 ft

in a transect spanning 691.0ft between MW1 and SG8 (Appendix B-7). Starting at MW1, the

probe was inserted into the ground and pushed through the silt and clay layers until refusal was

met. Typically refusal could be felt as contact with coarse gravel or cobbles. Multiple 5.0ft steel

rods could be threaded together if silt/clay thickness was greater than 5.0 ft. Once refusal was

met, the total amount of steel rod inserted into the ground was recorded and a tape measure was

used to determine the next probing point. A total of thirty two silt/clay thickness measurements

were made along the 691.0ft transect.

3.5. Vegetation mapping

Vegetation at the GTS was mapped visually and paired with several vegetation surveys.

The visual vegetation mapping focused on determining zones throughout the site in which

vegetation types were of similar species. Within each vegetation zone, vegetation survey plots were performed. These vegetation plots were performed by placing a 1.0 meter by 1.0 meter survey grid randomly throughout each vegetation zone seen in Figure 13 [Daubenmire R, 1959].

Figure 13: Vegetation survey plot being used at the GTS

Within each of these one square meter grids, all plant species present were recorded and percent

cover of each species was estimated. Additionally samples of each species in each plot were

taken and placed in labeled paper bags. These vegetation samples were brought to Montana

Technological University and reviewed with Professor Robert Pal (Department of Biological

Sciences, Montana Technological University) to confirm plant species type. Using the United

States Army Corps of Engineers "Wetland Indicator Rating", a wetland indicator value was

assigned to each zone. A Mann-Whitney U test was performed to determine which zones were

statistically different based off wetland indicator value.

3.6. Groundwater modeling

3.6.1. Computer program and code

Groundwater modeling was performed using the program Groundwater Modeling System (GMS) produced by Aquaveo, Inc. This program uses the USGS produced MODFLOW version 2000 finite difference code to model groundwater flow. GMS serves as the model program interface in which information is placed into and pulled from MODFLOW code.

3.6.2. Model domain

The model domain consists of a roughly 1,500 ft long by 1,100 ft wide grid. This domain features 10,860 active cells that are each 10 ft by 10 ft seen in Figure 14. The shape of the model domain is based off aerial LiDAR data imported into GMS from Geographic Information System (GIS). The grid is bounded by the mountain front to the west, MFJD to the east, Bear Creek to the north and the southern border is located where the valley aquifer narrows significantly. Grid cells were assigned top elevations based off the imported GIS LiDAR data. For a detailed description of how GIS LiDAR data was imported into GMS, see Appendix C-3.
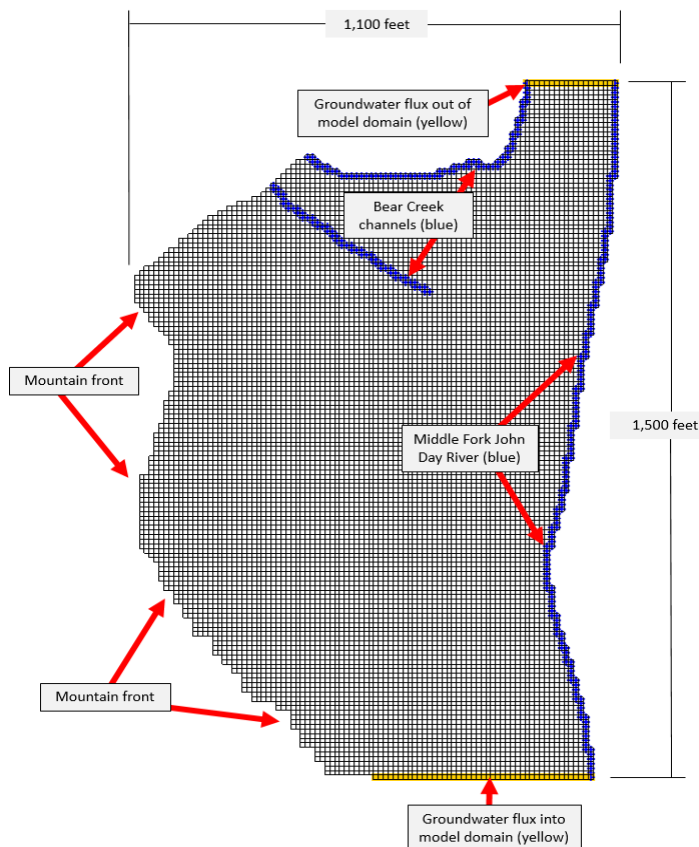
Figure 14: Model domain with relevant site features labeled.

3.6.3. Aquifer properties

3.6.3.1. Type and thickness

Based off the geologic conditions at the GTS, the valley aquifer was modeled as an unconfined aquifer. This aquifer was assumed to be 30.0 ft thick from available subsurface data (Table 1). Although this 30.0 ft thickness was used for the modeling, variation in model thickness was explored in the sensitivity analysis. The model consists of one layer, which represents the valley aquifer unit as well as the adjacent alluvial fan. The relatively thin silt and clay layers were not included in the groundwater model due to their observed discontinuous nature throughout the GTS.

3.6.3.2. Hydraulic conductivity and storativity

Two hydraulic conductivity values were used in the groundwater model. The alluvial fan sediments were given a hydraulic conductivity of 1.0 ft per day. This hydraulic conductivity was determined from slug tests performed in the alluvial fan sediments. The valley aquifer material was given a hydraulic conductivity of 70.0 ft per day. This hydraulic conductivity was determined from soil sieve analyses and Hazen's equation. An average hydraulic conductivity from the three separate soil sieve analyses was used.

Storativity of the valley aquifer and alluvial fan materials was estimated based off the hydraulic conductivity of the aquifer material and geology. These values were determined to be 0.15 and 0.05 respectively. These value falls within an acceptable range for their geologic composition and estimated hydraulic conductivity in reviewed literature [Fetter, 2014].

3.6.4. Boundary conditions

3.6.4.1. Middle Fork John Day River

The MFJD was modeled using the river package. River conductance was calculated using Equation 2. Inputs for Equation 2 came from measured MFJD width, a hydraulic conductivity similar to the aquifer sediment and an assumed aquifer thickness. The calculated river conductance was relatively high compared to the aquifer sediment indicating the aquifer sediment and water table will control whether water enters or leaves the MFJD. This works well in the context of the boundary conditions because the MFJD is a gaining stream throughout most of the GTS and simply allows groundwater to exit the model through the MFJD.

Equation 2: River conductance equation

$$C = \frac{wk}{t}$$

Where:
C = conductance (ft²/day)   w = width of river
k = hydraulic conductivity (ft/day)   t = thickness of river bed sediment

River stage inputs for the MFJD were acquired by predicting stage levels at the GTS

from USGS gauge station discharge values and manual stage measurements. Using these stage

predictions and LiDAR determined river bottom elevations.

3.6.4.2.   Restored Middle Fork John Day River

The final proposed restoration work on the MFJD calls for the construction of a main

meandering channel with several secondary channels. The geometry of these channels was

obtained from a HEC-RAS hydraulic model constructed by IFI. This hydraulic model contained

ground surface elevation data describing the post restoration site terrain as well as surveyed

sections throughout the GTS. These elevation data were imported directly into GMS to define

the top of the model and geometry of the new MFJD channels (Figure 15). In order to determine

stage in each respective channel of the re-designed MFJD, a hydraulic model was constructed

using Microsoft Excel. Using MFJD discharge records between May 10, 2018 and October 13,

2018, a discharge value was placed into the hydraulic model and the stage in all channels was

determined at that time. Whether or not secondary channels were active or not at a given

discharge was determined based off the bottom elevation of the main channel at the confluence

of that secondary channel, the stage in the main channel and the elevation of the bottom of the

secondary channel. Secondary channels were considered active when main channel stage was

high enough to exceed the bottom elevation of the secondary channel at a given discharge. In

order to determine stage in the main channel based off an input discharge, the Manning's

equation was used and is described in Equation 3 [Akan, 2006]. Manning's equation requires a Manning's roughness coefficient, channel width, discharge and channel slope to be input in order to determine channel stage. Manning's roughness coefficient, channel width and channel slope were all either measured or pulled from the IFI HEC-RAS model.

Equation 3: Manning's equation

$$Q = \left(\frac{1.49}{n}\right) A \, R^{\frac{2}{3}} \sqrt{S}$$

Where:
Q = discharge (ft³/day)
n = Manning's roughness coefficient
A = channel area (ft²)
R = channel hydraulic radius (ft)
S = channel slope (ft/ft)

The restored channels of the MFJD were all modeled in GMS using the river package. By using river package the restored channels of the MFJD could be simplified to head-dependent boundaries that supplied the proper amount of water to the aquifer. Given rivers typically act as groundwater hydraulic boundaries; channels east of the main channel of the restored MFJD were left out of the groundwater model. River conductance for these restored channels was relatively uncertain compared to other model inputs due to the fact that restoration will be performed with whatever sediment can be located on site. To account for this uncertainty in river conductance, a value of 1687.5 ft²/day or 25% lower than the river conductance value used in the pre-restored MFJD groundwater model was used. By using a lower river conductance, the river will be less capable of transferring water to the aquifer. Since the main question is whether or not enough water is supplied to the wetlands by the restored MFJD channels, a lower river conductance will produce a conservative estimate of the amount of water moving from the restored MFJD into the aquifer and subsequently the wetlands.

Two of the modeled secondary MFJD channels only flow from May 10, 2018 to June 19, 2018. In order to properly account for these channels no longer carrying flow with the river

package, the model was split into two models. The first model ran from May 10, 2018 to June 19, 2018 with both secondary MFJD channels simulated with river package. The second model ran from June 20, 2018 to October 13, 2018 with both secondary MFJD channels removed from the model. Removing the two channels from the model ensured that the river package did not properly apply head to the model when no flow was occurring in the channel. In order to tie the two models together transiently, the second model was given the initial head conditions from the last time step of the first model. This ensured that the second model started from where the first model ended and thus properly simulated the entire modeling period.
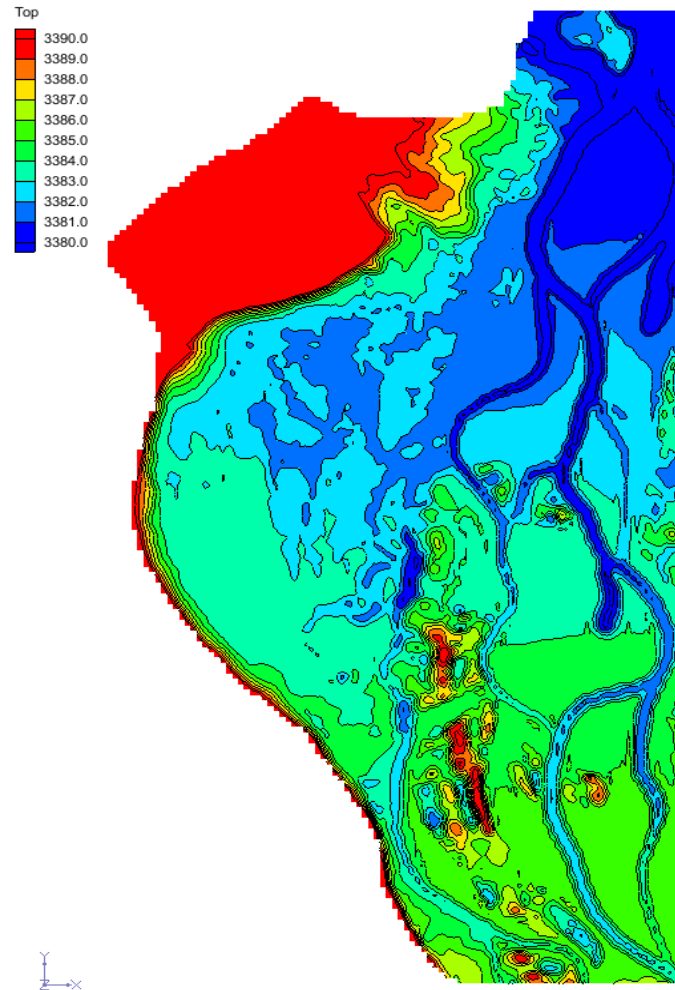
Figure 15: Ground surface elevations of the restored MFJD model domain.

3.6.4.3. Bear Creek

The channels of Bear Creek were all modeled using the river package. River conductance was relatively unknown compared to other model inputs for these channels however, a rough conductance was calculated using Equation 2 and conductance inputs seen in Table 3. The creek bed sediments in Bear Creek were visually observed as being slightly coarser than subsurface alluvial fan sediment. Given the large variation in river conductance, river conductance was used as a tool in model calibration in order to properly match observed water levels.

Stage inputs for Bear Creek were determined from manual discharge and stage measurements as well as from LiDAR determined stream bottom elevations. Appendix D-2 displays the stage values used for the various Bear Creek channels.

3.6.4.4. Groundwater flux

Groundwater fluxes into the south end of the model and out of the north end of the model were calculated using Darcy's Law (Equation 4). Cross sectional area was determined by measuring the valley width at each location and multiplying that by the aquifer saturated thickness of 26.0 ft. Hydraulic conductivity was assumed to be the same as the hydraulic conductivity of the aquifer sediment. Hydraulic gradients were measured from hand drawn water table contours based off observed water elevations. These hand drawn contours can be found in Appendix B-5. Table 4 displays the range of groundwater flux for each end of the model. The variability in the value of groundwater flux was considered in the model sensitivity analysis.

Equation 4: Darcy's Law

$$Q = -kA\frac{dh}{dl}$$

Where:
Q = flow rate (ft^3/day)
k = hydraulic conductivity (ft/day)
A = aquifer cross sectional area (ft^2)
$\frac{dh}{dl}$ = hydraulic gradient (ft/ft)

3.6.5. Initial conditions (steady-state model)

The initial conditions for the transient model and subsequent predictive models were derived from a steady state model based off GTS conditions on July 9, 2018. Boundary condition inputs for Bear Creek, MFJD and groundwater flux were acquired from field measurements and performed calculations. Observation points were given a 0.75 ft target calibration range based off the 7.5 ft of head drop across the site. The model was run several times using Bear Creek river conductance as the primary calibration tool.

3.6.6. Flow Budget

In order to determine how modeled flows in and out of the model domain compared to real-world estimated flows in and out of the model domain, a flow budget analysis was performed. Modeled in and out flows were determined directly from the GMS model outputs for the steady-state model.

Real-world estimated in and out flows were determined from surface flow data and hand-drawn water table contours. The MFJD was assumed to be gaining throughout most the entire reach and thus only considered a groundwater flow output. An estimation of groundwater flow into the MFJD was determined by measuring the length of the MFJD at the site and saturated aquifer thickness from nearby staff gauges and wells. A rough hydraulic gradient near the MFJD was determined from hand-drawn water table contours maps. Finally the aquifer hydraulic conductivity was acquired from soil sieve analyses. Using these inputs, a rough flow of groundwater into the MFJD was determined using Darcy's Law. On the date of the steady-state model (July 9, 2018) all flow from Bear Creek was into the wetlands and thus was considered a groundwater input. Flow into the groundwater from Bear Creek was determined using measured discharge measurements of Bear Creek upstream of the wetlands. Finally groundwater fluxes in

and out of the real-world estimated flow budget were determined with the methodology described in Section 3.6.4.4.

3.6.7. Sensitivity analysis

In order to assess the sensitivity of the model to different model inputs, an extensive model sensitivity analysis was performed on the steady state model. MFJD conductance, Bear Creek Channel B conductance, Bear Creek conductance, groundwater flux in, groundwater flux out and hydraulic conductivity were all allowed to vary -50%, -25%, 0%, 25% and 50% from their initial input. Additionally model thickness was varied -33%, 0% and 33% from its initial input.

3.6.8. Transient (unsteady) model

The transient model or unsteady state model was set to simulate GTS conditions from May 10, 2018 to October 13, 2018. Daily stress periods were used throughout the modeling period, producing a total of 156 stress periods. These stress periods were broken into eight 3.0 hour time steps. Boundary condition inputs for Bear Creek, MFJD and groundwater flux were acquired from field measurements and performed calculations. Observation points were given a 0.8 ft target calibration range which was calculated as 10% of the total 8.0 ft head drop across the site during the transient period. The transient model was run several times using logical adjustments in Bear Creek stage during periods where actual conditions on Bear Creek were not observed.

3.6.9. Predictive models

3.6.9.1.   Pre-Restoration

In order to determine the impact of restoration work on the wetlands, a predictive model

simulating the conditions that would have occurred over the entire monitoring period if no

restoration was constructed. This required allowing Bear Creek channel B to continue normal

base flow conditions after late-July. In reality after late-July, restoration work decreased Bear

Creek Channel B flow dramatically. Since no data exist on Bear Creek channel B flow between

late-July and October, the characterized flow relationship between Bear Creek's main and

channel B as well as the recorded base flow prior to restoration were used to determine the

theoretical stage in channel B [Appendix D-2]. This model provided a baseline of conditions at

the site, and specifically the wetlands, prior to any restoration work. The water table elevation

data from this model will be used in comparison with models simulating restored conditions.

3.6.9.2.   Complete Bear Creek Removal

Proposed restoration plans call for the complete removal of flow in channel B. Observed

post-restoration conditions showed that although dramatically reduced, flow in channel B

persisted. In order to properly determine the total impact of removing channel B flow into the

wetlands, an additional model was constructed to simulate site conditions if channel B was

completely removed. Since channel B was completely removed, the appropriate amount of water

was added to the main Bear Creek channel to account for water no longer flowing down channel

B. The water table elevation data from this model will be used in comparison with pre-

restoration water elevations to determine the complete impact of Bear Creek restoration on the

GTS.

3.6.9.3. Post-Restoration

The final model ran for this investigation simulated the conditions following the completion of all proposed restoration work. This includes removal of channel B, re-meandering of MFJD, construction of new secondary channels on the MFJD, and grading throughout the site. This grading ultimately raises MFJD channel elevations on the east portion of the site. Section 3.6.4.2 describes how restored MFJD channel inputs were obtained. Bear Creek inputs were the same as the model in which Bear Creek channel B was completely removed as described in section 3.6.9.2. The water table elevations from this model were used to determine the overall impacts of all proposed restoration work on the GTS.

3.6.10. Predictive Model Uncertainty

In order to address model uncertainty in certain parameters, several post-restoration models were constructed with varying values of hydraulic conductivity and specific yield. By varying these parameters a range of water table elevations indicative of post-restoration conditions were created. These water table elevations were used to determine average and maximum gain or drop in water table elevation caused by varying either hydraulic conductivity, specific yield or both simultaneously. Water table elevation changes were observed at MW6 because this point is located near the wetlands and showed the most sensitivity to changes in hydraulic conductivity and specific yield.

4. Results

4.1. Groundwater

4.1.1. Hydrographs

Recorded water elevations levels in all the equipment over the entire monitoring period, May 10, 2018 through October 13, 2018 are transposed in Figure 16. During this period of time, 15 pieces of monitoring equipment dried up in late July 2018 and stayed dry through September 2018. Appendix B-4 shows relative change in head for each piece of monitoring equipment for the entire monitoring period. All water elevation data can be found in Appendix B-2 and B-3 in tabular form.

In addition to tabular and graphical data, water elevation was used to construct several water contour maps. Appendix A shows rough groundwater contours as well as groundwater flow direction for June 23, 2018 and July 9, 2018 respectively.
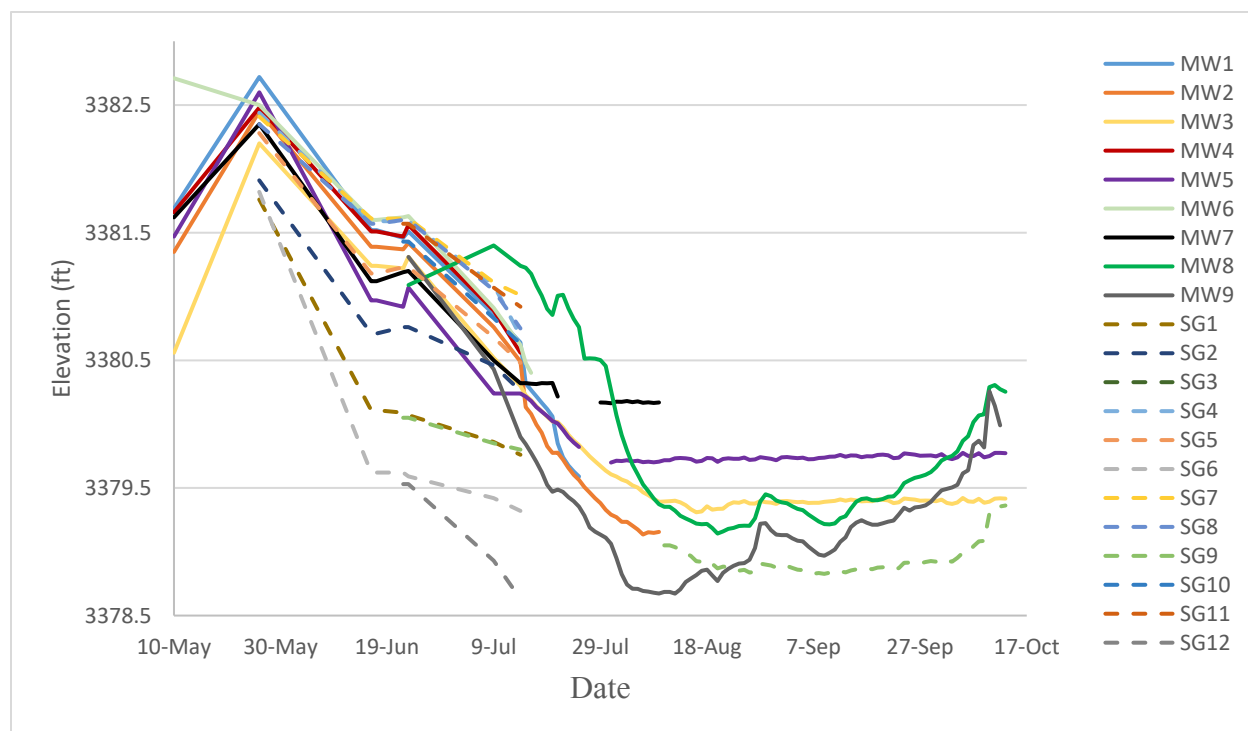
Figure 16: Water elevations in monitoring equipment between May 10, 2018 and October 13, 2018. Monitoring wells are solid lines, staff gages are dashed lines.

Temperature and specific conductivity measurements taken with the Multi 340i probe are in Appendix B-6. Transducer recorded temperature data is available upon request.

4.2. Surface water flows

4.2.1. Middle Fork John Day and Bear Creek

Bear Creek discharge measurement results can be seen in tabular form in Appendix B-10. MFJD discharge measurements were made by the USGS gauge station for the entire period of monitoring. MFJD discharge measurements made on the same days as Bear Creek discharge measurements can be seen in Appendix B-10. Figure 17 shows a combined hydrograph of both MFJD and Bear Creek during the period of monitoring.

4.3. Hydraulic conductivity
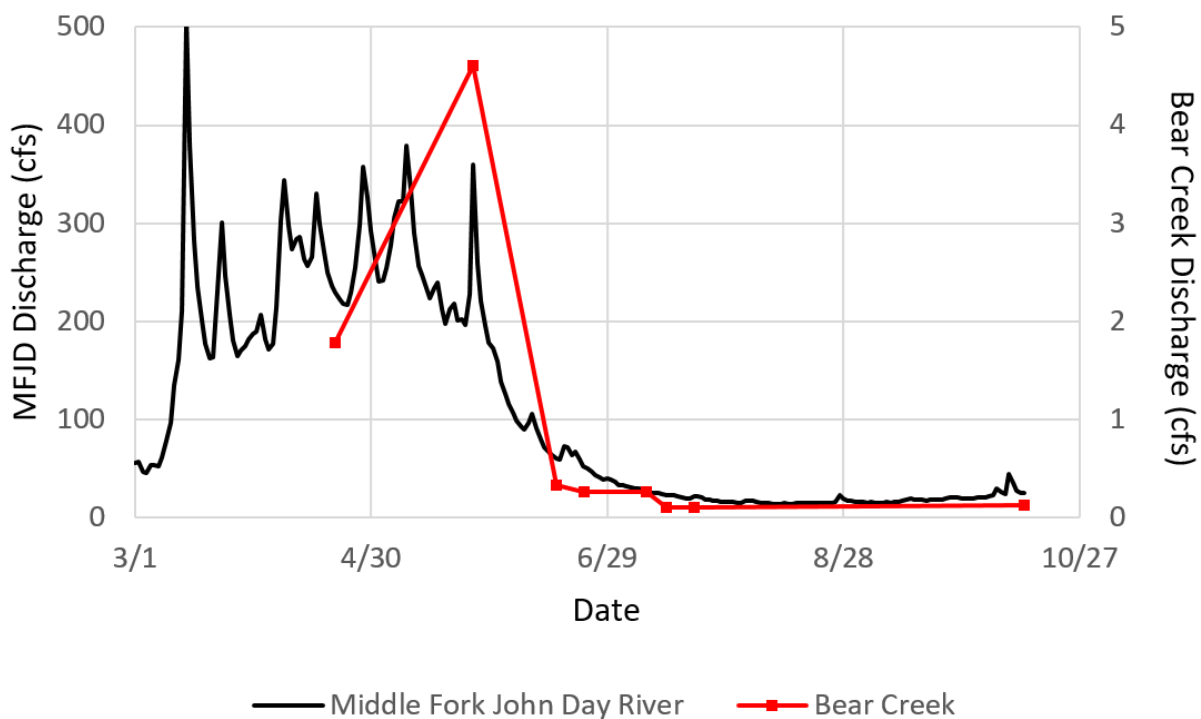
Figure 17: Combined discharge measurements of the MFJD (black) and Bear Creek (red) capturing high flow levels on the MFJD. Left vertical axis depicts MFJD discharge and the right vertical axis depicts Bear Creek discharge.

Hydraulic conductivity results showing slug test data and Hvorslev estimation lines are in Appendix C-2. These tests produced a range of hydraulic conductivity for the silt/clay layer and alluvial fan sediments as seen in Table III.

Raw sieve analysis data and particle size distribution curves for each sample are in Appendix C-1. Using the Hazen equation and several equation constants, these samples produced a range of hydraulic conductivities for the gravel aquifer seen in Table III.

Table III: Hydraulic conductivity results by test and geologic unit

Location	Test #	Test Type	Geologic Unit	Low hydraulic conductivity estimate (ft/day)	High hydraulic conductivity estimate (ft/day)
MW1	1			0.01	0.05
MW3	1		Silt/clay layer	0.03	0.10
	2			0.03	0.03
	3	Hvorslev slug test		0.02	0.02
MW8	1		Alluvial fan sediment	0.55	1.57
MW9	1		Silt/clay layer	0.05	0.11
	2			0.03	0.47
	3			0.02	0.12
MW6	1	Sieve analysis w/ Hazen's equation	Sand, gravel, cobble aquifer material	20.4	61.2
	2			36.3	108.9
	3			41.0	122.9

Combining all of these hydraulic conductivity analyses produces ranges of hydraulic conductivity for each of the three geologic units; clay/silt, sandy silt and aquifer gravel. Table IV summarizes these hydraulic conductivity results based off geologic unit.

Table IV: Summary of hydraulic conductivity data based off geologic unit

Geologic unit	Range of hydraulic conductivity (ft/day)
Silt/clay layer	0.01 - 0.12
Alluvial fan sediment	0.55 - 1.57
Sand, gravel, cobble aquifer material	20.4 - 122.9

4.4. Silt/clay layer thickness

Raw silt/clay layer thickness data can be seen in tabular form in Appendix B-8. Figure 18 shows a cross section view of this transect. Typically silt/clay thickness ranged from 0.2 ft to 5.0 ft. Generally the silt/clay unit is thicker on the south end of the site near MW1, shallower near MW6 and deepens again in the wetlands near SG8 on the north end of the site.
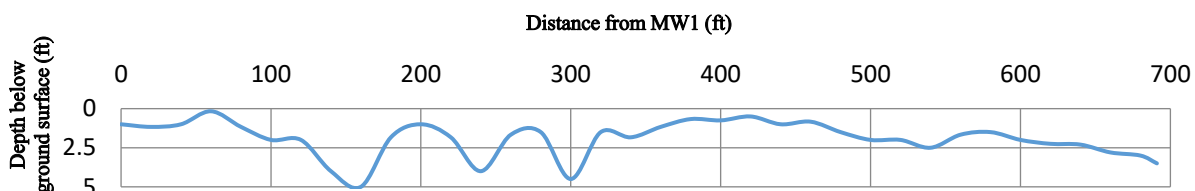
Figure 18: Total depth of silt/clay layer below ground surface from MW1 to SG8

4.5. Vegetation mapping

Seven different vegetation zones were mapped, the extents of which are shown in Figure 19. Eight total vegetation plots were performed throughout these vegetation zones and twenty total plant species were encountered. Vegetation species data can be seen in Table V. The site was dominated by non-native grasses and showed phreatophytes (water loving plants) exclusively in the wetlands area. When comparing native and exotic species in each zone, it was found that zones 2, 3, and 4 are dominantly natives while zones 1, 5, and 6 are dominantly exotic (Figure 20). When applying wetland indicator values based of species presence to each zone, zones 1, 2 , 4, 5, and 6 are all given a relatively low wetland indicator value and are not statstically different from one another (Figure 21). Zone 3 was given a high wetland indciator value and was noted as being statistcally different than all the other zones. Given zone 3 makes up the wetland area, a high wetland indicator value is expected.
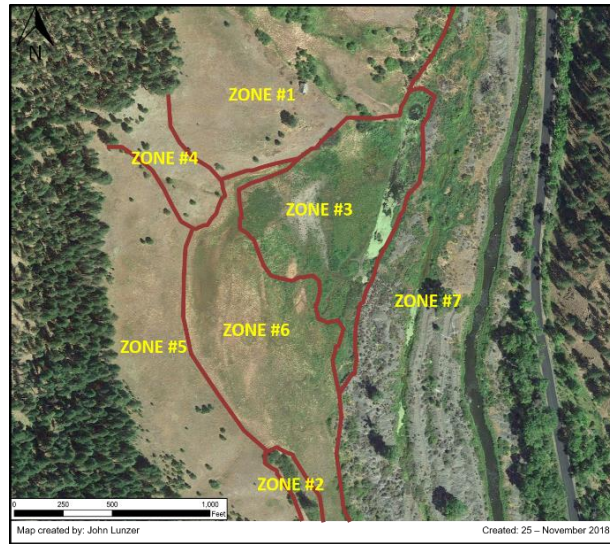
Figure 19: Map showing the location and extent of each vegetation zone at the GTS.

Table V: Species present in each zone and plot.

Zone	Plot number	Species common name	Species Latin name	% Cover
1	1	Holboell's rockcress	*Boechera holboellii*	3.0
		Yarrow	*Achillea millefolium*	10.0
		Moss	----	10.0
		Creeping foxtail	*Alopecurus arundinaceus*	45.0
		Smooth brome grass	*Bromus inermis*	22.0
		Litter	----	10.0
	2	Lupin	*Lupinus*	1.0
		Yarrow	*Achillea millefolium*	1.0
		Smooth brome grass	*Bromus inermis*	60.0
		Wildrye	*Elymus repens*	28.0
		Litter	----	10.0
2	----	Black locust	*Robinia pseudoacacia*	----
3	1	Sedge	*Carex nebrascensis*	1.0
		Bentgrass	*Agrostis stolonifera*	5.0
		Perennial bunchgrass	*Phalaris arundinacea*	70.0
		Litter	----	20.0
	2	Beaked sedge	*Carex rostrata*	65.0
		Litter	----	30.0
	3	Curly dock	*Rumex crispus*	12.0
		Beaked sedge	*Carex rostrata*	40.0
		Creeping yellowcress	*Rorippa sylvestris*	5.0
		Litter	----	40.0
4	1	Wild rose	*Rosa woodsii*	1.0
		Smooth brome grass	*Bromus inermis*	10.0
		Thickspike wheatgrass	*Agropyron dasystachyum*	30.0
		Litter	----	50.0
5	1	Yarrow	*Achillea millefolium*	4.0
		Wild rose	*Rosa woodsii*	1.0
		Timothy-grass	*Phleum pratense*	20.0
		Smooth brome grass	*Bromus inermis*	30.0
		Litter	----	30.0
6	1	Prairie smoke	*Geum triflorum*	1.0
		Cinquefoil	*Potentilla gracilis*	5.0
		Timothy-grass	*Phleum pratense*	85.0
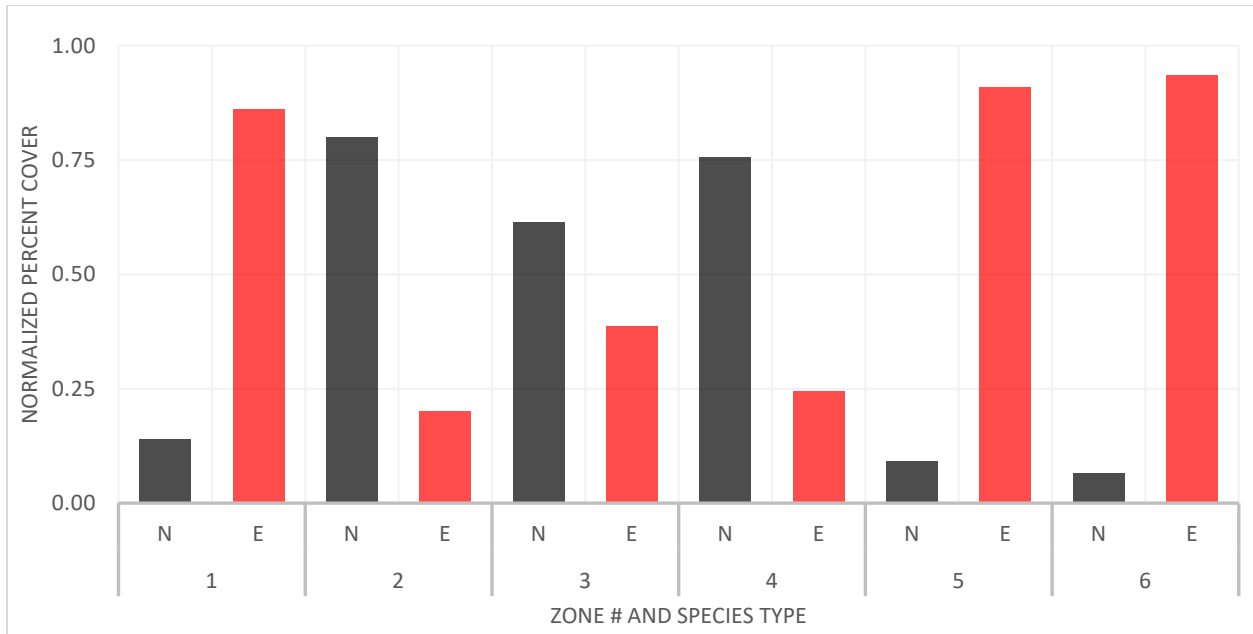
Figure 20: Normalized percent cover of native (N) and exotic (E) species for each mapped vegetation zone
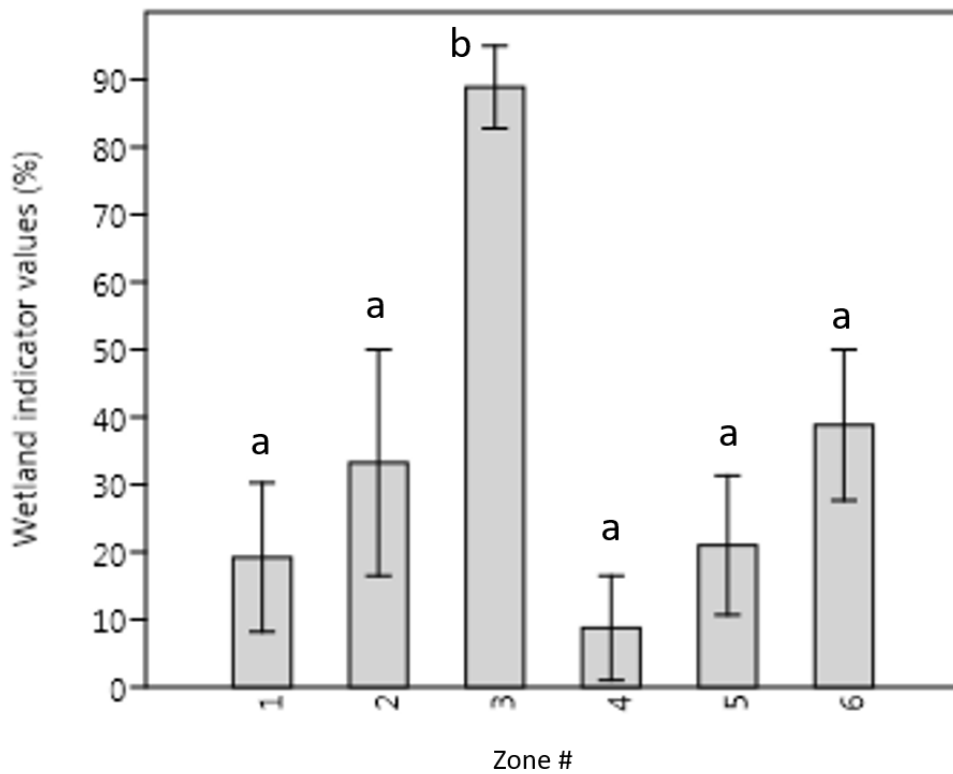
Figure 21: Wetland indicator value for each mapped vegetation zone. (a) zones and (b) zones are statistically different from one another.

4.6. Groundwater modeling

4.6.1. Boundary conditions inputs

Tables VI and VII show the boundary conditions inputs for river conductance and

groundwater flux respectively. All other model inputs can be found in Appendix D.

Table VI: River conductance inputs for MFJD and Bear Creek

Input	MFJD	Bear Creek
Hydraulic conductivity (ft/day)	70.0	5.0
Width of river (ft)	25.0	5.0
Thickness of river bed sediment (ft)	0.5 – 1.0	0.2 – 0.5
Calculated conductance (ft^2/day)	1750.0 – 3500.0	50.0 – 125.0

Table VII: Darcy law inputs for groundwater flux (south and north boundaries)

Input	South boundary	North boundary
Hydraulic conductivity (ft/day)	70.0	70.0
Aquifer cross sectional area (ft^2)	11,000	4,750
Hydraulic gradient (ft/ft)	0.004	0.004
Flow rate (ft^3/day)	2917.9	1400.0

4.6.2. Steady state model

The steady-state model ran for July 9, 2018 produced water table contours seen in Figure 22. This model was well-calibrated producing an observed vs. modeled chart seen in Figure 23. Additionally this chart shows the absolute mean error and root mean squared error (RMS error) as 0.31 ft and 0.37 ft respectively.
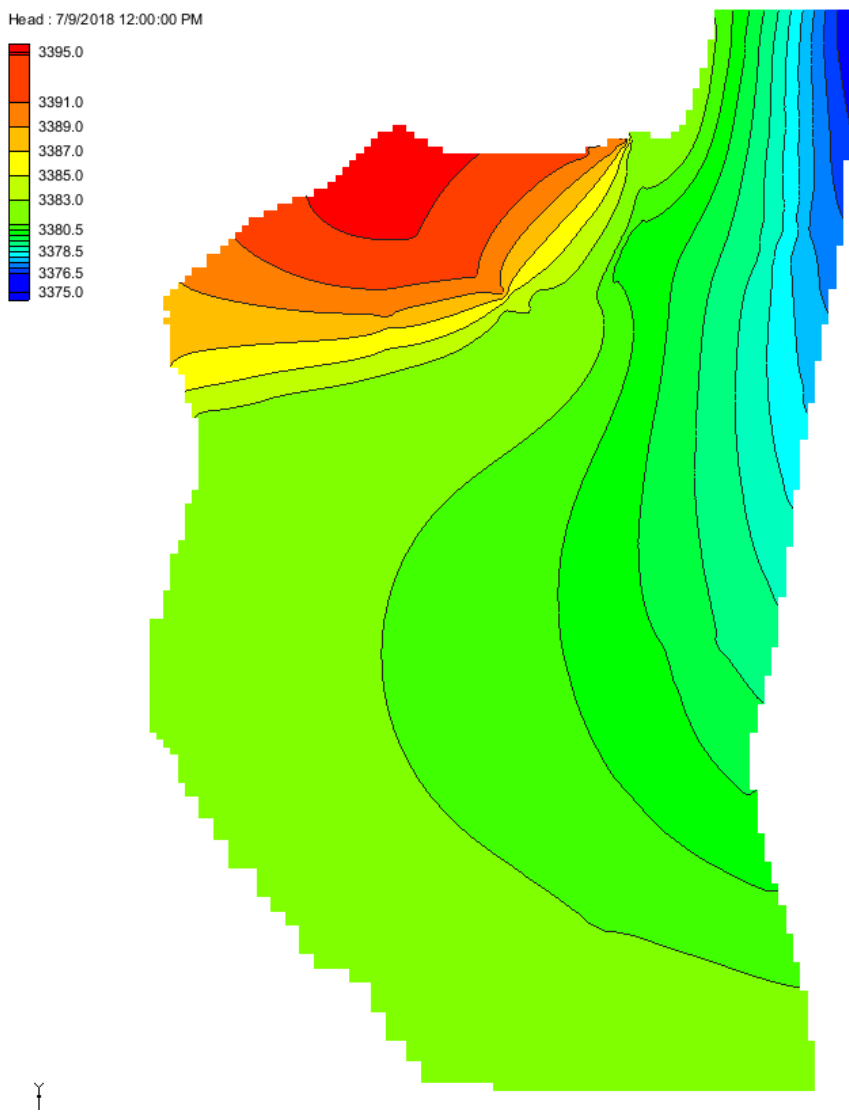
Figure 22: Head contours for the July 9, 2018 steady state model.
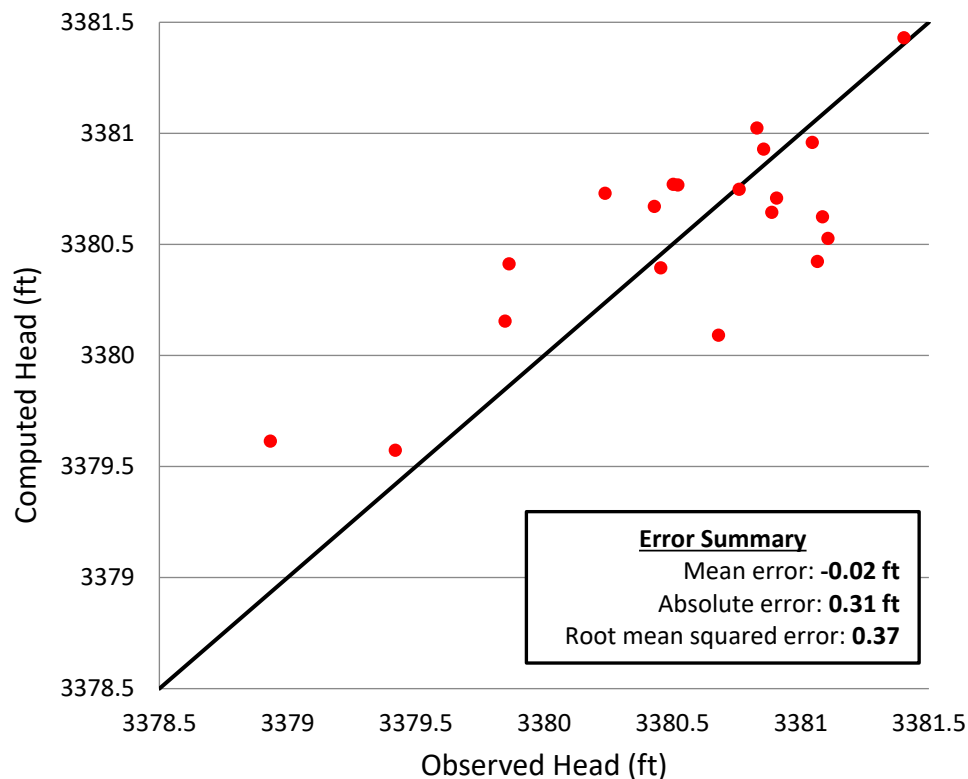
Figure 23: Computed vs. observed head plot and error summary for the July 9, 2018 steady state model.

4.6.3. Flow budget

Tabular and graphical data displaying estimated and modeled in- and outflows can been

seen in Table VIII and Figure 24. Modeled inflow was 619.2 cubic feet per day (cfd) more than

estimated inflow or 2.42% of total estimated inflow. Modeled outflow was 273.2 cfd greater than

estimated outflow or 1.07% of total estimated outflow.

Table VIII: Steady state model flow budget estimated and modeled values.

	Estimated		Modeled		Difference	
Source	**Inflow**	**Outflow**	**Inflow**	**Outflow**	**Inflow**	**Outflow**
MFJD River(ft³/day)	0	24,500.0	53.8	24,764.8	53.8	264.8
Bear Creek (ft³/day)	22,636.8	0	23,201.5	8.4	564.7	8.4
Groundwater flux	2917.9	1400.0	2917.9	1400.0	0	0
Total(ft³/day)	25,554.7	25,900.0	26,173.9	26,173.2	619.2	273.2
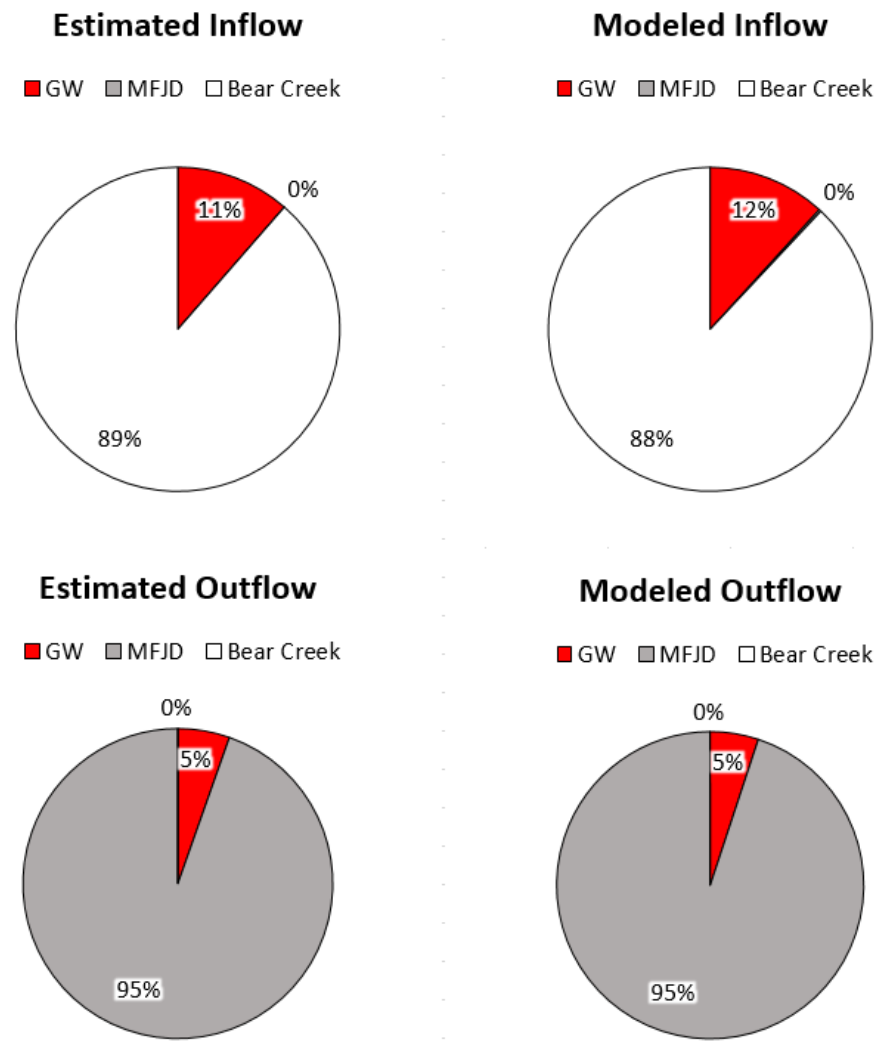
Figure 24: Pie charts depicting estimated and modeled inflows and outflows.

4.6.4. Sensitivity analysis

Figure 25 shows change in RMS error for each model parameter based off percent change in that particular model parameter. The plot shows that the main channel of Bear Creek conductance (main channel consists of channels A, C, D, E and F in Figure 11), MFJD conductance, groundwater flux into the model and groundwater flux out of the model have relatively low impact on the error in the model. Bear Creek (Channel B) has a moderate impact

on model error. Finally hydraulic conductivity and model thickness have a significant impact on model error.
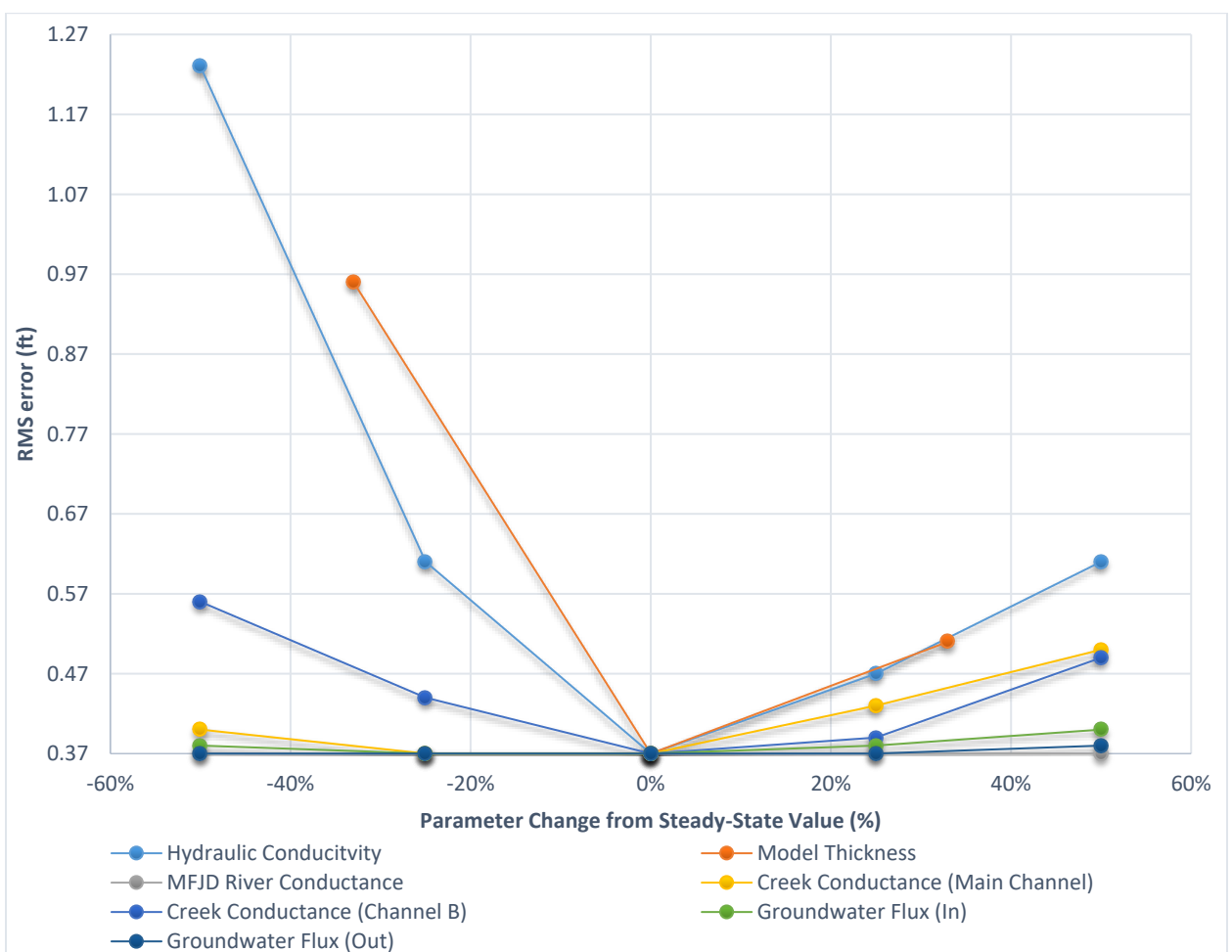
Figure 25: Sensitivity plot depicting RMS error vs. percent change in parameter.

4.6.5. Transient model

Figure 26 shows water elevation levels over time plots at four different locations throughout the site. The gray lines on these plots indicate the modeled water elevation, the white dots show the observed values, the boxes show the difference between modeled and observed and the brackets how the calibration target range. If a box is green the modeled water elevation falls within the calibration target range, if the box is yellow the modeled water elevation is within two times the calibration target range and if the box is red the modeled water elevation is

outside of two times the calibration target range. Generally all modeled water elevations fall

within the calibration target range throughout the entire model, MW8 and MW9 represent the

two observation points in the transient model with the most modeled water elevations outside the

calibration target range. Error for the transient model seen on Figure 26 shows a mean error of -

0.03 ft, an absolute error of 0.44 ft and a RMS error of 0.52 ft for the entire transient model.

4.6.6. Predictive models

Water elevations from all three predictive models were used to create water elevation

plots for four separate observations points throughout the model domain. Figure 27 shows the

location of these four observations points; MW1, MW6, SG9 and WET. Figure 28 shows the

four water elevations at all four observation points for the observed, pre-restoration, complete

removal of Bear Creek channel B, and post MFJD restoration models.
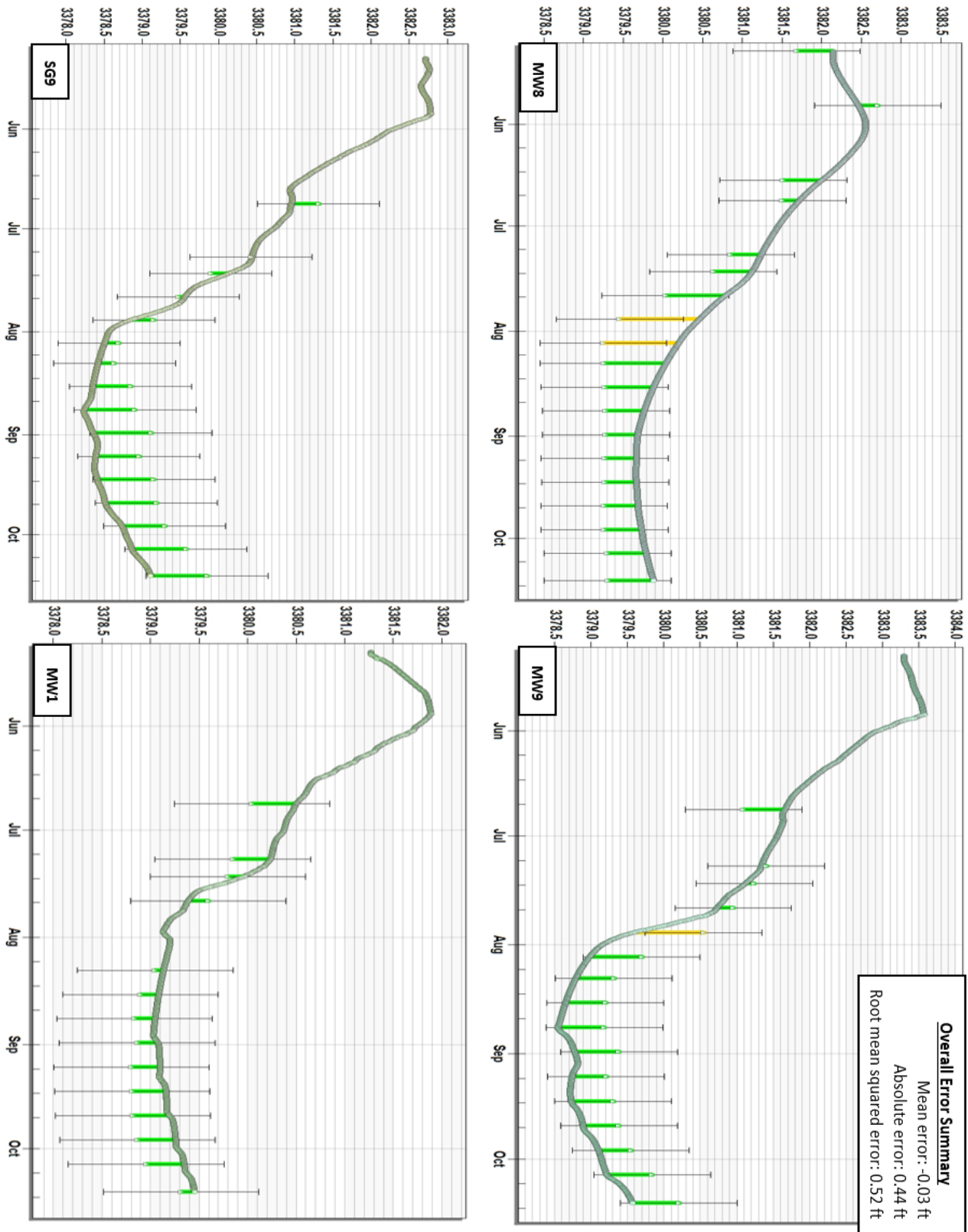
Figure 26: Transient model modeled water elevation plots, calibration target range and error summary.
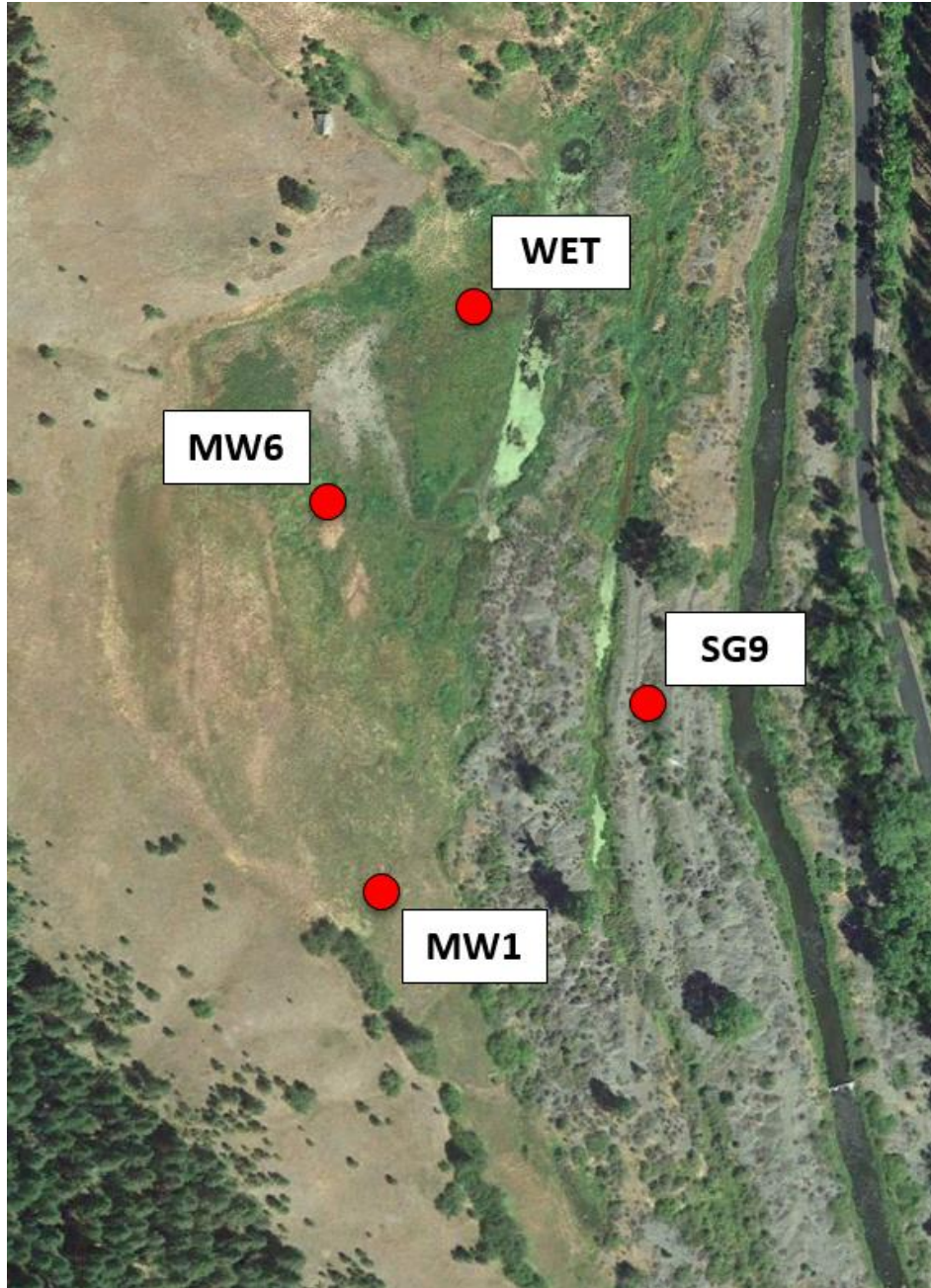
Figure 27: Four locations selected throughout the site where modeled water elevations were plotted to determine the impacts of restoration across the site.
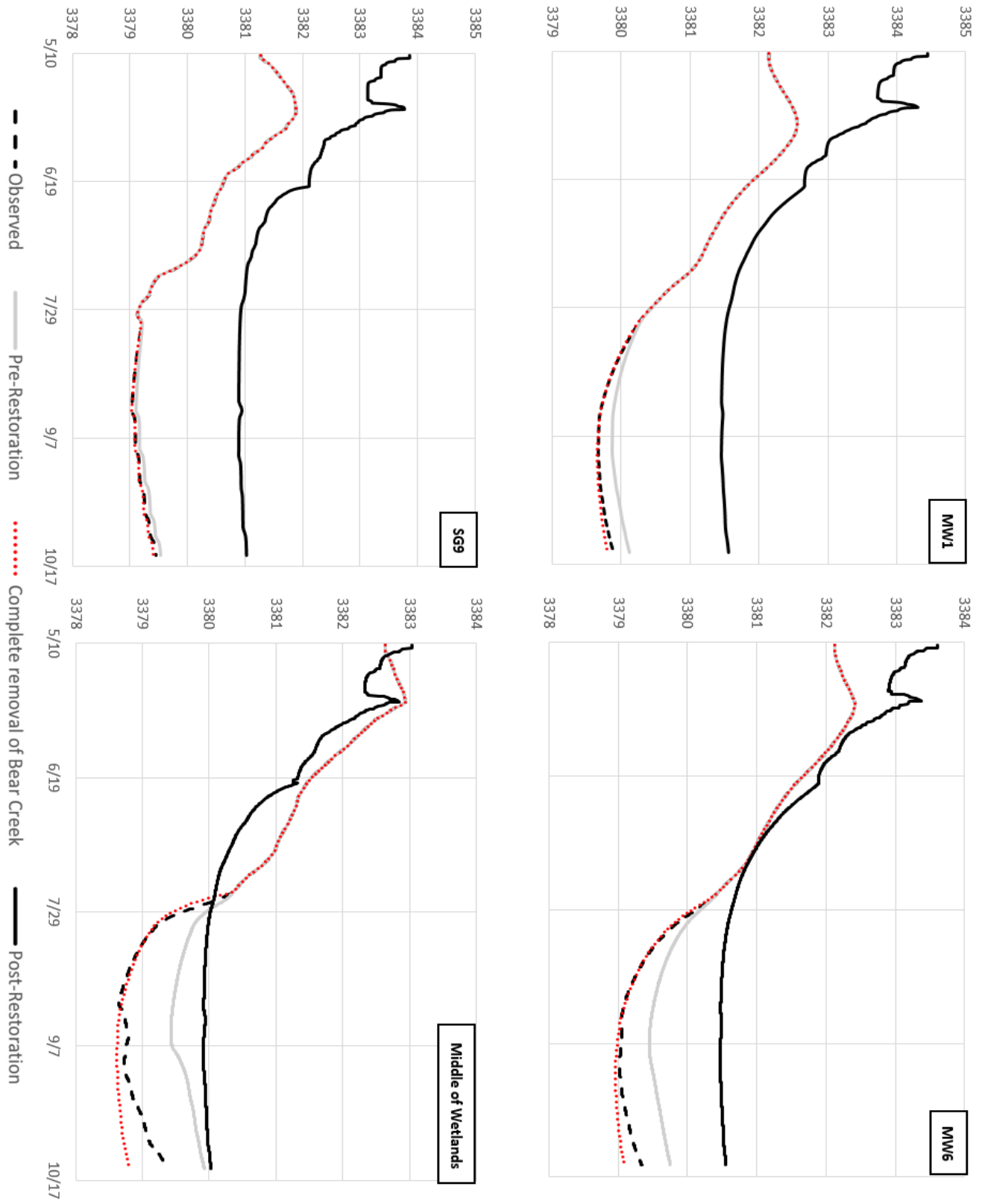
Figure 28: Predictive model water elevation plots.

4.6.7. Predictive model uncertainty

In order to quantify uncertainty of the predictive model, hydraulic conductivity and specific yield were adjusted by -71.4%, 0.0%, 71.4% and -67.0%, 0.0%, 67.0% respectively. Table IX shows the results of the uncertainty analysis in terms of hydraulic conductivity and specific yield values input into the model and the subsequent average and maximum impact on water elevations at observation point MW6 relative to the post MFJD restoration model water elevations. Overall out of the eight total models ran, four showed a rise in water elevation and four showed a lowering of water elevation at MW6.

Table IX: Predictive model uncertainty analysis

Run	Hydraulic conductivity (ft/day)	Specific yield	Average change to water elevation (ft)	Maximum change (ft)
1	70	0.25	0.09	0.26
2	20	0.15	0.35	0.79
3	20	0.25	0.66	1.01
4	20	0.05	0.10	0.23
5	120	0.15	-0.10	-0.26
6	120	0.25	-0.03	-0.04
7	70	0.05	-0.09	-0.42
8	120	0.05	-0.13	-0.59

5. Discussion

5.1. Groundwater modeling

5.1.1. Steady state and transient model error

Overall both the steady state and transient models produced RMS errors of 0.37 ft and 0.52 ft respectively. These RMS errors both fall within 10% (0.8 ft) of the total head drop across the flat portion of the model. Additionally only three observed water elevations fall outside the calibration target range of 0.8 ft throughout the entire transient model. These low RMS error values and overall well-calibrated nature of the models indicate that model inputs and parameters are relatively accurate.

5.1.2. Sensitivity analysis

The steady state model sensitivity analysis results seen in Figure 23 reveal the model is the most sensitive to hydraulic conductivity and model thickness. Hydraulic conductivity in particular is the parameter the model is most sensitive to due to the control hydraulic conductivity has one flow rates through the model. Given the wide range of experimentally determined hydraulic conductivities described in section 4.3, hydraulic conductivity was applied in the predictive model uncertainty analysis. This allowed for quantification of how impactful hydraulic conductivity is on the predictive model results.

5.1.3. Predictive model uncertainty

As seen in Table 8 in section 4.6.6, varying hydraulic conductivity and specific yield has varying degrees of impact on predictive model results. Inputting a hydraulic conductivity of 20 ft/day and specific yield of 0.25 produced a maximum increase in modeled water elevation at MW6 of 1.08 ft. Inputting a hydraulic conductivity of 120 ft/day and specific yield of 0.05 produced a maximum decrease in modeled water elevation at MW6 of 0.593 ft. Essentially this

shows that if the predictive model hydraulic conductivity and specific yield are both significantly differ from the true value, the model will predict water elevations that are within under a foot of the originally predicted water elevations. Given the uncertainty of hydraulic conductivity and specific yield as well as the sensitivity of the model to these parameters, the lack of significant change in predicted water elevations increases confidence of model water elevation results and subsequent predictions.

5.1.4. Evapotranspiration

Evapotranspiration was not considered in this model domain for several reasons; (1) limited site data regarding evapotranspiration rates throughout the site. (2) a significant amount of the site area is currently bare, waste rock material which has no vegetation and are unsaturated. (3) the amount of water leaving the model domain through evapotranspiration is relatively small compared to other model inputs and outputs. This amount was determined with a rough conservative approximation from available USGS "Annual average evapotranspiration rates" [USGS, 2019]. The results of this rough approximation can seen below (Table X).

Table X: Rough approximation of domain evapotranspiration

Parameter	Units	Value
Average annual ET rate per year [USGS]	(m/yr)	0.396
	(ft/yr)	1.299
	(ft/day)	0.0036
Model area	(ft^2)	1,089,900
Estimated waste rock area	(ft^2) (ft^2)	300,000
Total area contributing to ET	(ft^2)	789,900
Volume of water removed from ET	(cfd)	2843.64
Percent of total modeled outflow	(%)	10.86
Average drop in water elevation across model	$(ft/ft^2/day)$	0.0026

5.2. Model predictions

Figure 26 (section 4.6.5) reveals the impacts of restoration throughout the GTS. Both MW1 and SG9 show post-restoration water elevations being significantly higher than pre-restoration water elevations throughout the entire modeling period. MW6 shows a similar trend although the magnitude of water elevation increase between pre- and post-restoration conditions is not as high. Finally the observation point in the middle of the wetlands (WET) shows a slight reduction in water elevations post-restoration from pre-restoration conditions from May 13 until July 28. This drop in water elevation is at its greatest magnitude of 0.69 ft on July 10. After July 28, the post-restoration model shows an increase in water elevation at WET from pre-restoration conditions. All four water elevation plots show a drop in water elevations in the post-restoration model after June 19 when flow into secondary channels of MFJD ceases, reducing water supply to much of the domain.

Post-restoration conditions overall increase the water elevations from pre-restoration conditions across the model domain. In particular, MW6 will have surface water present three more days out of the modeling period compared to pre-restoration conditions. A reduction in water elevations can be observed in the portion of the wetlands nearest the location of abandoned Bear Creek Channel B during the May to July period. This is likely due to the fact that during pre-restoration conditions, Bear Creek Channel B input a significant amount of surface water to the aquifer during the May to July period. This significant input of surface water to the aquifer produced a groundwater mound near the mouth of channel. In the post-restoration conditions, Bear Creek Channel B no longer inputs surface water to the aquifer and the pre-restoration groundwater mound is flattened out producing the lower modeled water elevations for May through July in this location. This flattening of the groundwater mound means at location WET,

surface water will be present eight fewer days out of the modeling period compared to pre-restoration conditions.

5.3. Vegetation predictions

Based off the groundwater mode predictions, two general trends are anticipated for site vegetation; (1) as water elevations rise from restoration, vegetation zone 3 is expected to grow. Higher water levels in zone 6 will allow wetland adapted species found in zone 3 to spread. (2) this spread of wetland adapted species will cause the wetland indicator value for zone 6 to rise significantly as species with a higher wetland indicator value spread into the zone. (3) as species adapted to wetlands spread into zone 6, the zone will change from exotic dominated to native dominated. This is due to the fact that native species perform better in the wetland area than exotics.

6. Conclusions

Model error, sensitivity and uncertainty were all described and quantified well. Any uncertainty in sensitive parameters was accounted for in the analysis of predictive model uncertainty which revealed changes to sensitive parameters having relatively little impact on model results. The constrained nature of the model produced this lack of sensitivity to drastic changes. When comparing pre-restoration to post-restoration modeled conditions across the GTS, an overall increase in water elevations across the model domain is observed. In regards to the wetland area, a decrease in water elevation is observed near the abandoned Bear Creek Channel B, however, an increase in water elevation is observed in portions of the wetlands further from this abandoned channel. Post-restoration conditions will overall increase the extent of the wetland area across the model domain.

7. Recommendations

1. Perform further testing at the site to better characterize hydraulic conductivity and specific yield of the aquifer material. This will help lower overall uncertainty in model predictions.

2. Continue to monitor groundwater conditions during and after all restoration work is completed. This will allow for the ability to post-audit the groundwater model to further lower predictive uncertainty.

3. Monitor wetland vegetation between now and when work on the MFJD restoration work begins. With Bear Creek Channel B currently cut off from the wetlands, several seasons of low water conditions might negatively impact wetlands plant species and warrant replanting efforts after MFJD restoration is complete.

8. References Cited (or Bibliography)

Akan, O., 2006. Open Channel Hydraulics. 1st ed, Elsevier/BH.

ASTM D6913, 2017. Standard Test Methods for Particle-Size Distribution (Gradation) of Soils Using Sieve
Analysis. American Society for Testing and Materials International.

Baird, K.J., Stromberg, J.C. & Maddock, T., 2005. Linking riparian dynamics and groundwater: an
Ecohydrologic approach to modeling groundwater and riparian vegetation. Environmental Management, pp
551-564.

Boano, F. et al., 2006. Sinuosity-Driven Hyporheic Exchange in Meandering Rivers. Geophysical Research Letters,
vol. 33, no. 18.

Brown, E., and Thayer, P., 1966. Geologic Map of the Canyon City Quadrangle, Northeastern Oregon. United States
Geological Survey.

Daubenmire R., 1959 A Canopy-Coverage Method of Vegetational Analysis. Northwest Science Association.

Day, T.J., 1976. On the Precision of Salt Dilution Gauging. Journal of Hydrology 31: 293-306.

Department of Geology and Mineral Industries, 1957. Oregon's Gold Placers. State of Oregon.

Fetter, C.W., 2014. Applied Hydrogeology. 4th ed., Pearson.

Fleckenstein, Jan, et al., 2004. Managing Surface Water-Groundwater to Restore Fall Flows in the Cosumnes River.
Journal of Water Resources Planning and Management, vol. 130, ser. 4.

Groot S., de Graaff B., Oosterhoff C., Medenblik J., 2008. The Regge River: from canalized to meandering. Notes,
pp. 1983-1990.

Hongve, D., 1987. A Revised Procedure for Discharge Measurement By Means of the Salt Dilution Method.
Hydrological Processes 1: 267-270.

Kasahara, T. and Hill, A., 2008. Modeling the Effects of Lowland Stream Restoration Projects on Stream–
Subsurface Water Exchange. Ecological Engineering, vol. 32, no. 4, pp. 310–319.

Lindgren, W., 1901. The Gold Belt of the Blue Mountains of Oregon. United States Geological Survey.

Oregon Bureau of Land Management, 2019. Watershed Boundaries Oregon. State of Oregon.

Oregon Water Resources Department, 2019. Public Well Records. Well Report Query – State of Oregon.

Rogiers, B., Lermytte, J., De Bie, E. and Batelaan, O., 2011. Evaluating the impact of river restoration on the local groundwater and ecological system: a case study in NE Flanders. Geologica Belgica, vol. 14 (3-4), pp. 265-276.

Schneider, P., et al., 2011. Towards Improved Instrumentation for Assessing River-Groundwater Interactions in a Restored River Corridor. Hydrology and Earth System Sciences, vol. 15, no. 8, pp. 2531–2549.

Department of Geology and Mineral Industries, 2010. Susanville Quad LiDAR Data from Oregon Department of Geology and Mineral Industries. State of Oregon.

Svensson, A., 2014. Estimation of Hydraulic Conductivity from Grain Size Analyses. Chalmers University of Technology.

Uma, K.O., et al., 1989. New Statistical Grain-Size Method for Evaluating the Hydraulic Conductivity of Sandy Aquifers. Journal of Hydrology.

United States Geological Survey, 2019. USGS 14043840 MF JOHN DAY RIVER ABV CAMP CREEK, NR GALENA, OR. United States Geological Survey.

United States Geological Survey, 2019. USGS Seasonal Cumulative ET Anomaly data, United States Geological Survey.

U.S. Climate Data, 2018. John Day, Oregon Climate Monthly Data. United States Climate Data.

Winter, R., 2014. A Practical Application of Salt Tracer Injections. Montana Technological University.

9. Appendix A – Site Data
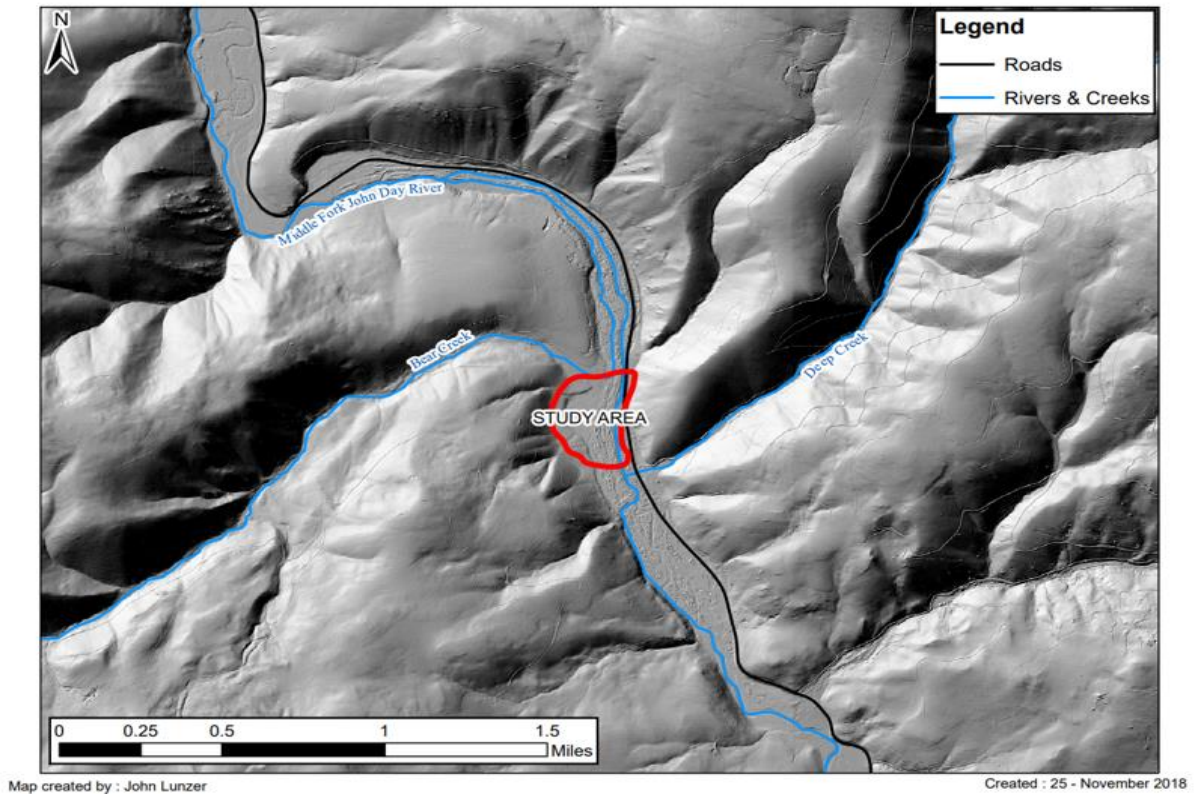
Appendix A-1: LiDAR derived DEM imagery for study area [State of Oregon].
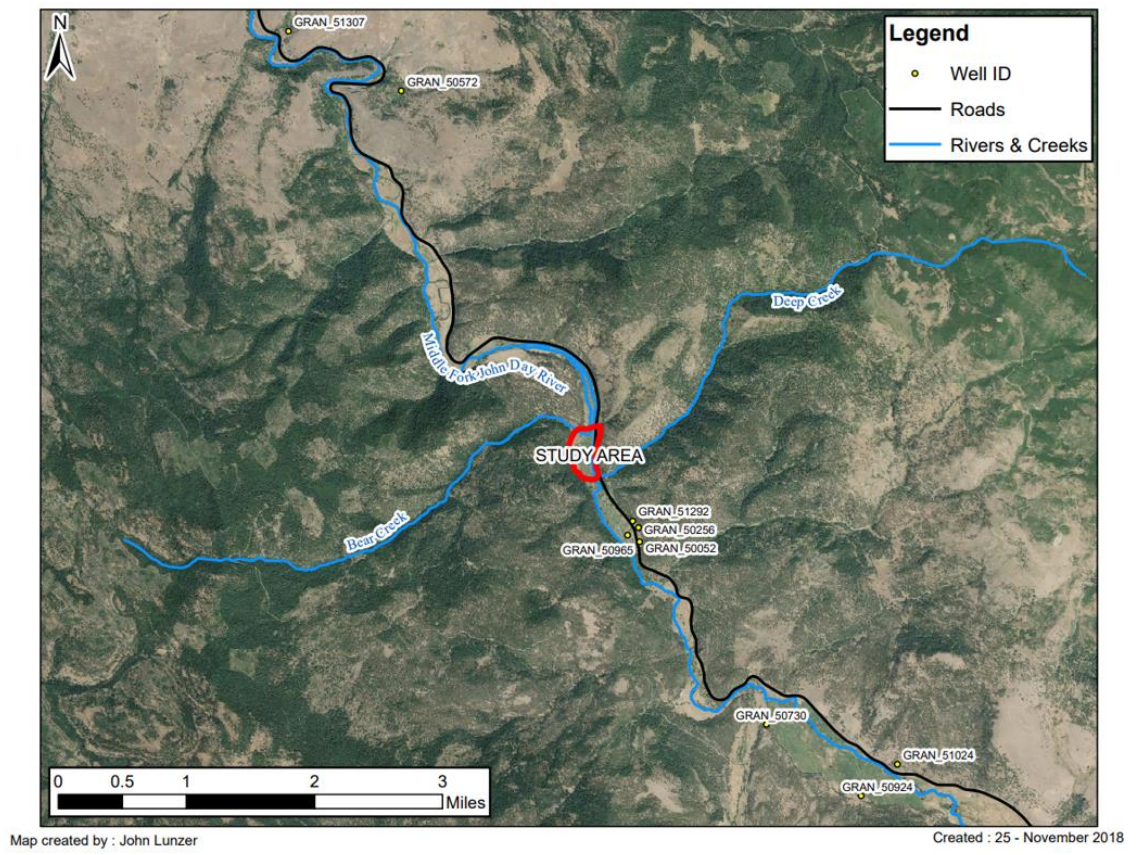
Appendix A-2: Locations of publicly available well logs relative to the study area [State of Oregon].

10. Appendix B – Monitoring and Field Data

Well ID:	MW1	Drilled by:	John Lunzer	Date installed:	5/10/2018
Drilled with:	Hand auger	Logged by:	John Lunzer	PVC Diameter:	1.0 inch

Geologic log & well construction diagram
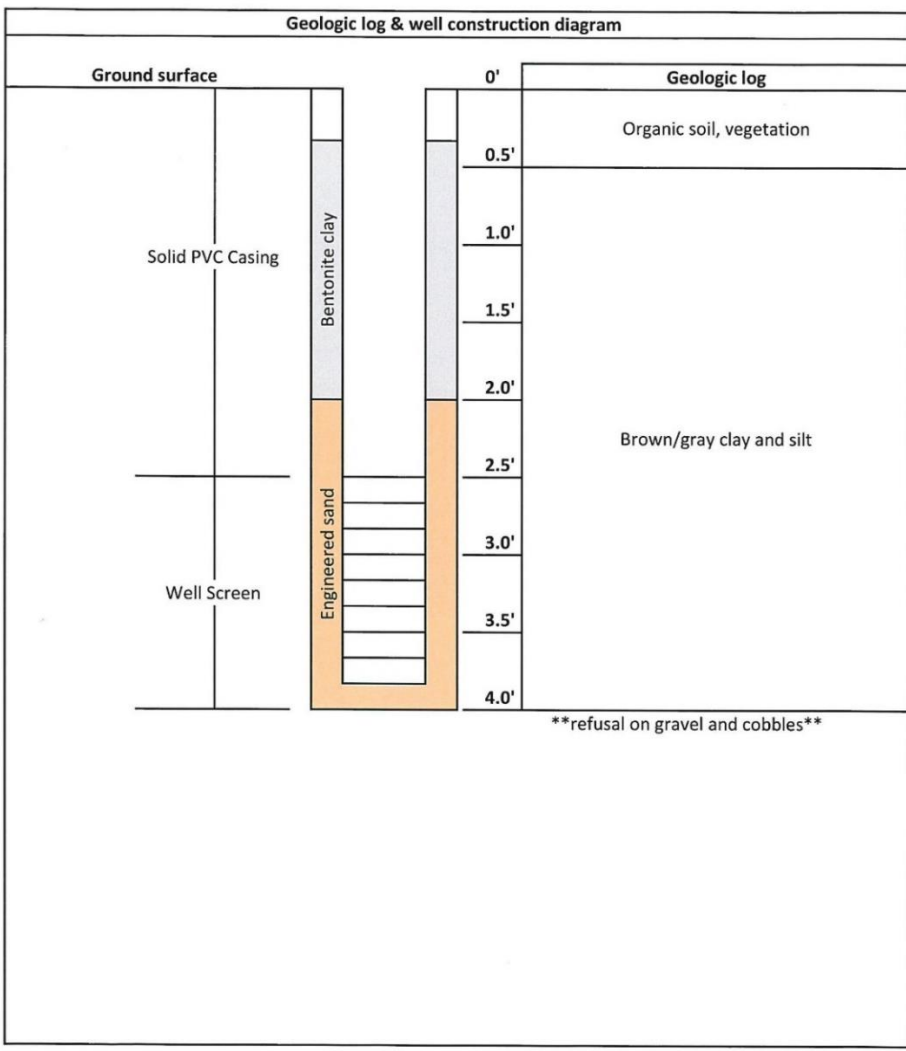
Appendix B-1-1: Geologic and well construction log for MW1.

| Well ID: | MW2 | Drilled by: | John Lunzer | Date installed: | 5/10/2018 |
| Drilled with: | Hand auger | Logged by: | John Lunzer | PVC diameter: | 1.0 inch |

Geologic log & well construction diagram
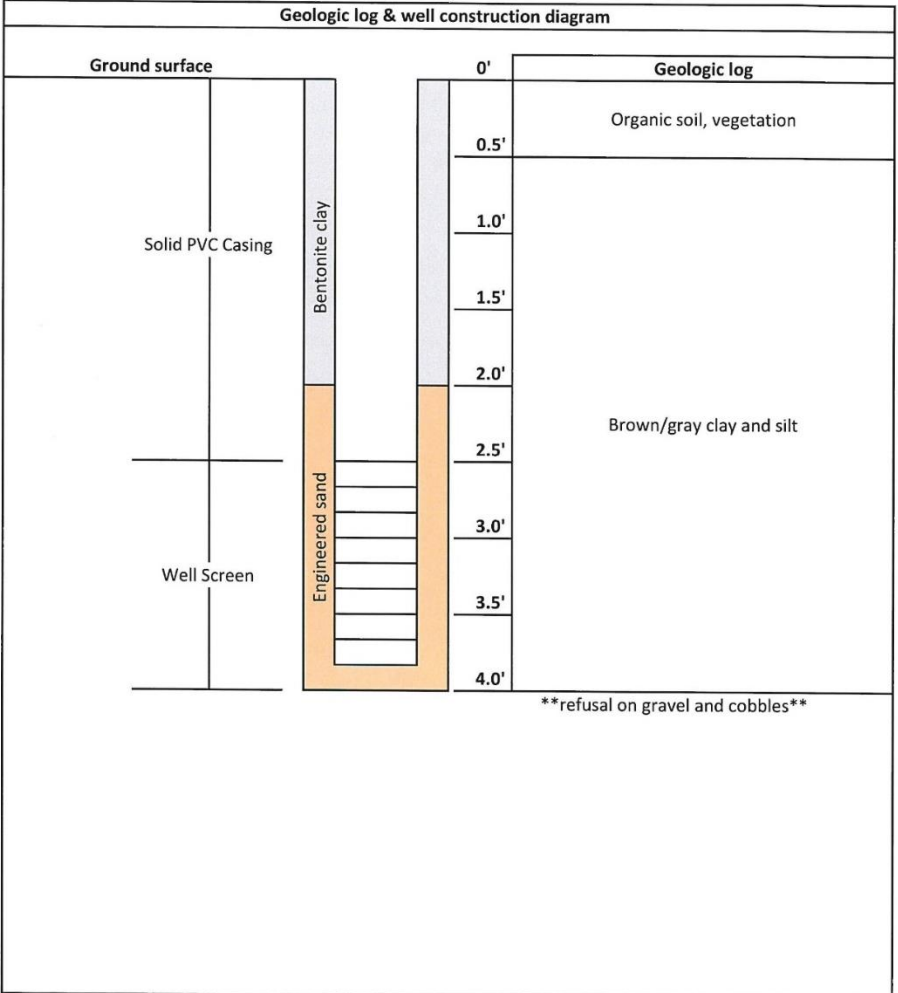
Appendix B-1-2: Geologic and well construction log for MW2.

Well ID:	MW3	Drilled by:	John Lunzer	Date installed:	5/10/2018
Drilled with:	Hand auger	Logged by:	John Lunzer	PVC diameter:	1.0 inch

Appendix B-1-3: Geologic and well construction log for MW3.

| Well ID: | MW4 | Drilled by: | John Lunzer | Date installed: | 5/10/2018 |
| Drilled with: | Hand auger | Logged by: | John Lunzer | PVC diameter: | 1.0 inch |

Geologic log & well construction diagram

| Ground surface | | 0' | Geologic log |

Clay

Solid PVC Casing — 0.5' — Organic soil, vegetation

Engineered sand

1.0'

Well Screen — 1.5' — Brown/gray clay and silt

2.0'

2.5'

refusal on gravel and cobbles

Appendix B-1-4: Geologic and well construction log for MW4.

Well ID:	MW5	Drilled by:	John Lunzer	Date installed:	5/10/2018
Drilled with:	Hand auger	Logged by:	John Lunzer	PVC diameter:	1.0 inch

Geologic log & well construction diagram

Ground surface		0'	Geologic log
Bentonite clay		0.5'	Organic soil, vegetation
Solid PVC Casing		1.0'	
Engineered sand		1.5'	
		2.0'	Brown/gray clay and silt
Well Screen		2.5'	
		3.0'	
			refusal on gravel and cobbles

Appendix B-1-5: Geologic and well construction log for MW5.

Well ID:	MW6	Drilled by:	John Lunzer	Date installed:	5/10/2018
Drilled with:	Hand auger	Logged by:	John Lunzer	PVC diameter:	1.0 inch

Geologic log & well construction diagram

Ground surface		0'	Geologic log
	Clay		Organic soil, vegetation
Solid PVC Casing		0.5'	
	Engineered sand	1.0'	
Well Screen		1.5'	Brown/gray clay and silt with sand
		2.0'	
			refusal on gravel and cobbles

Appendix B-1-6: Geologic and well construction log for MW6.
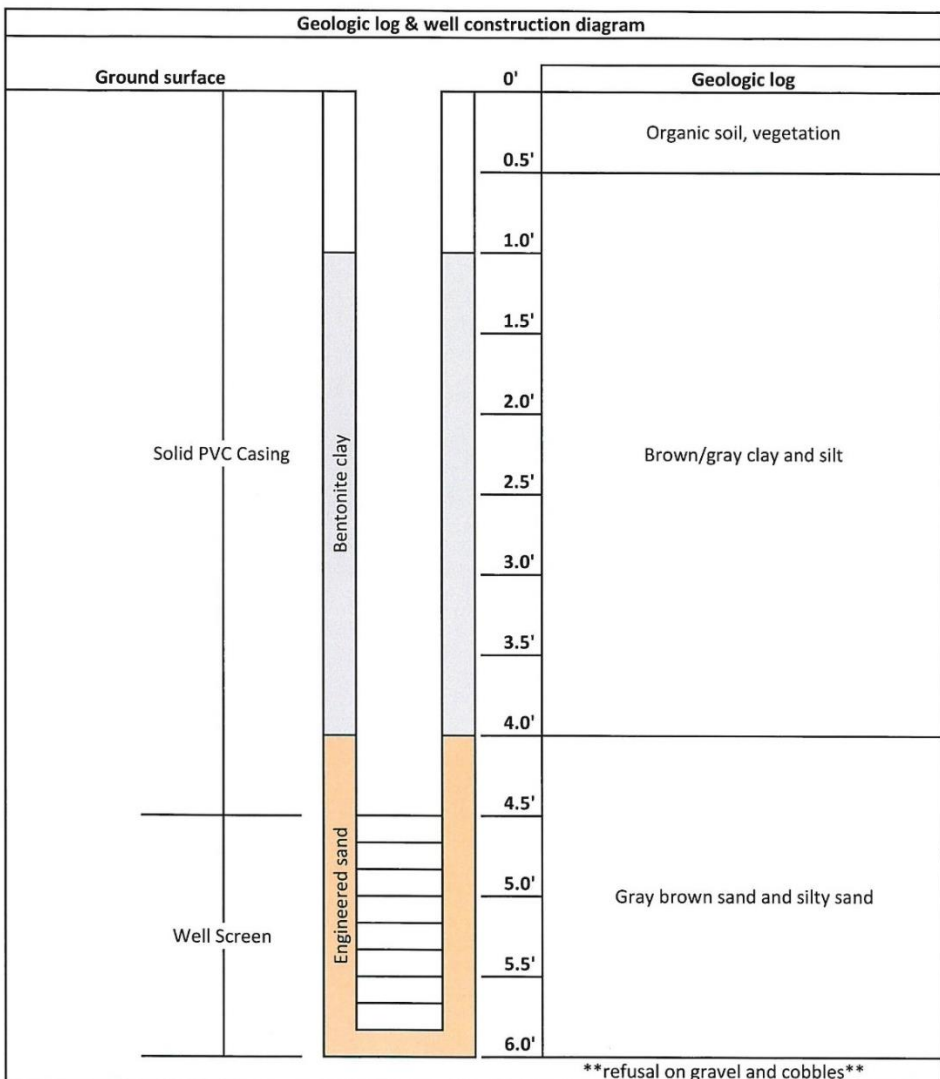
| Well ID: | MW7 | Drilled by: | John Lunzer | Date installed: | 5/10/2018 |
| Drilled with: | Hand auger | Logged by: | John Lunzer | PVC diameter: | 1.0 inch |

Appendix B-1-7: Geologic and well construction log for MW7.

Well ID:	MW8	Drilled by:	John Lunzer	Date installed:	6/23/2018
Drilled with:	Hand auger	Logged by:	John Lunzer	PVC diameter:	1.0 inch

Geologic log & well construction diagram

Ground surface — Solid PVC Casing — Bentonite clay — Engineered sand — Well Screen

Geologic log:
- 0' – 0.5': Organic soil, vegetation
- 0.5' – 3.0': Brown sandy silt with gravel
- 3.0' – 4.0': Brown/gray clay and silt with sand
- **refusal on gravel and cobbles**

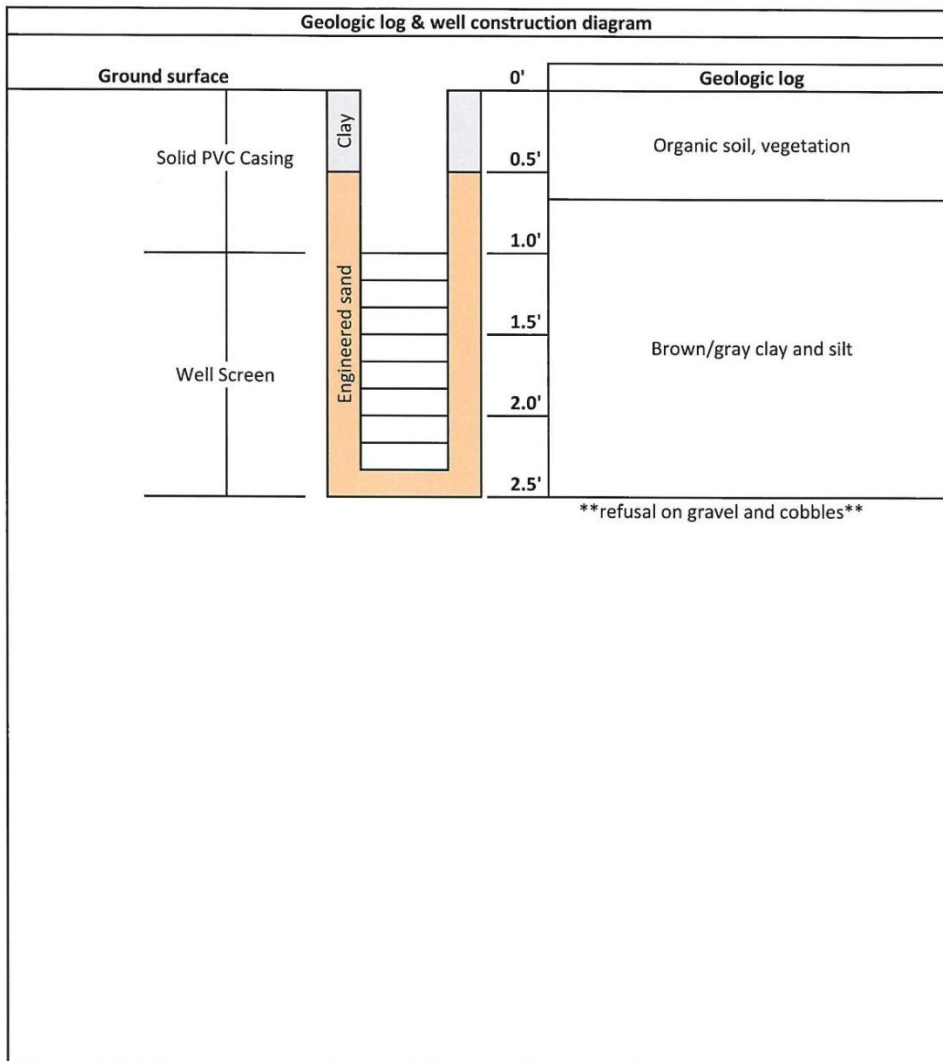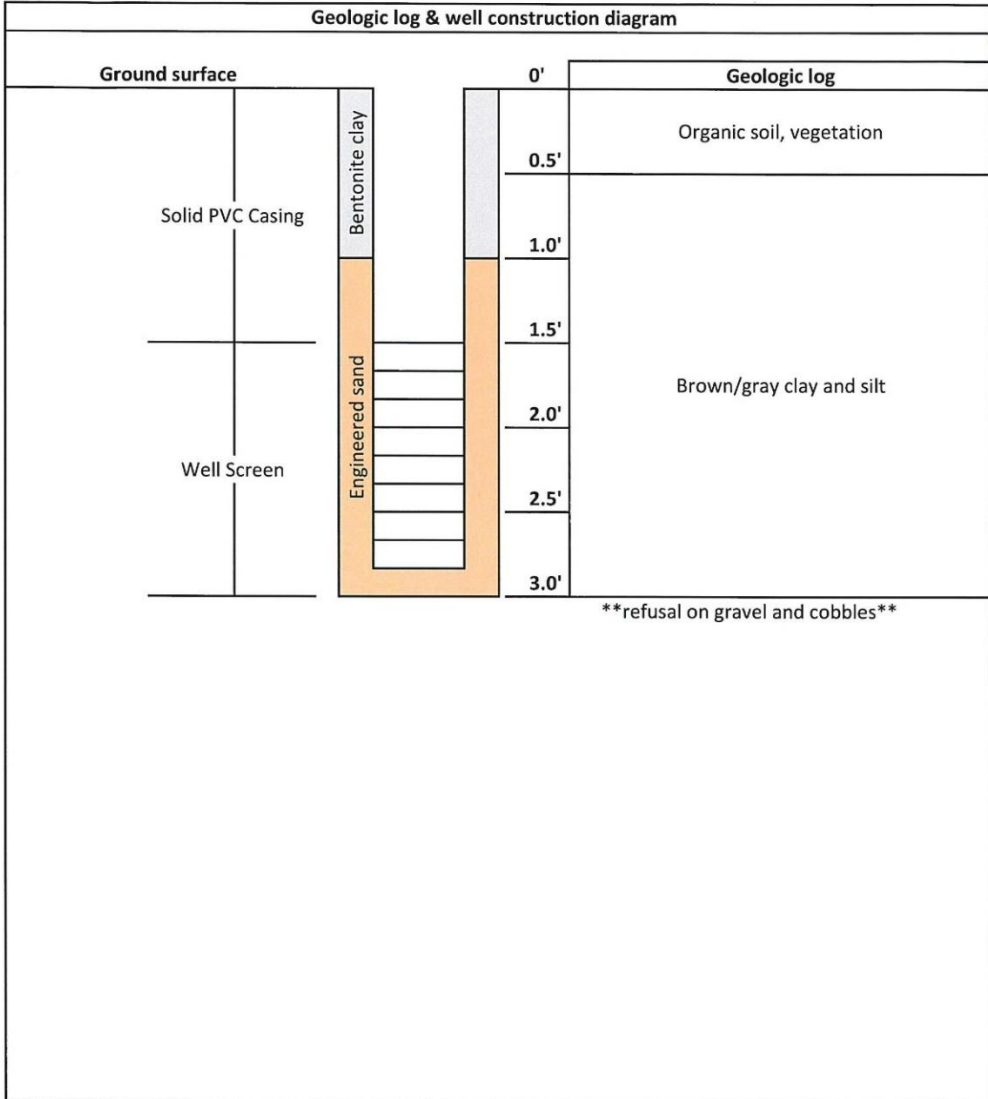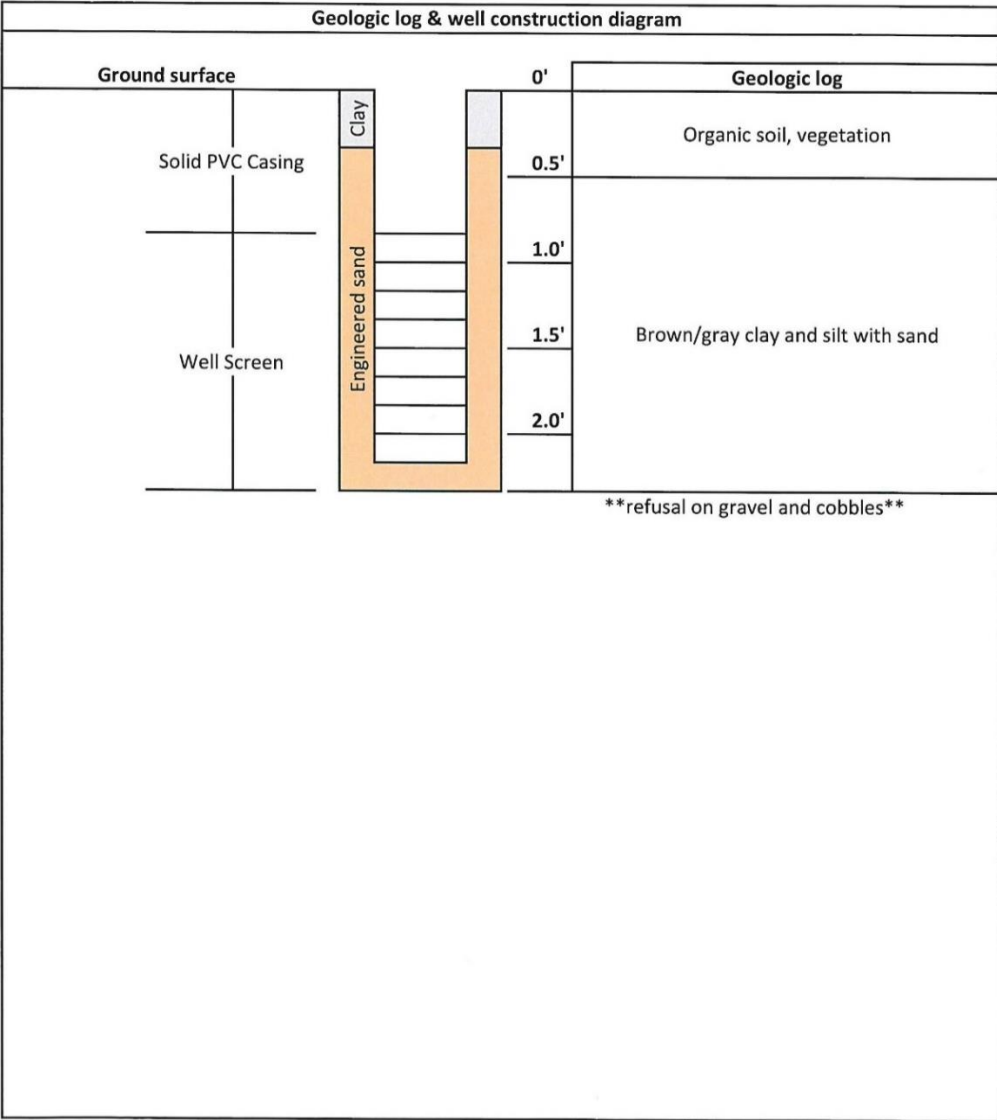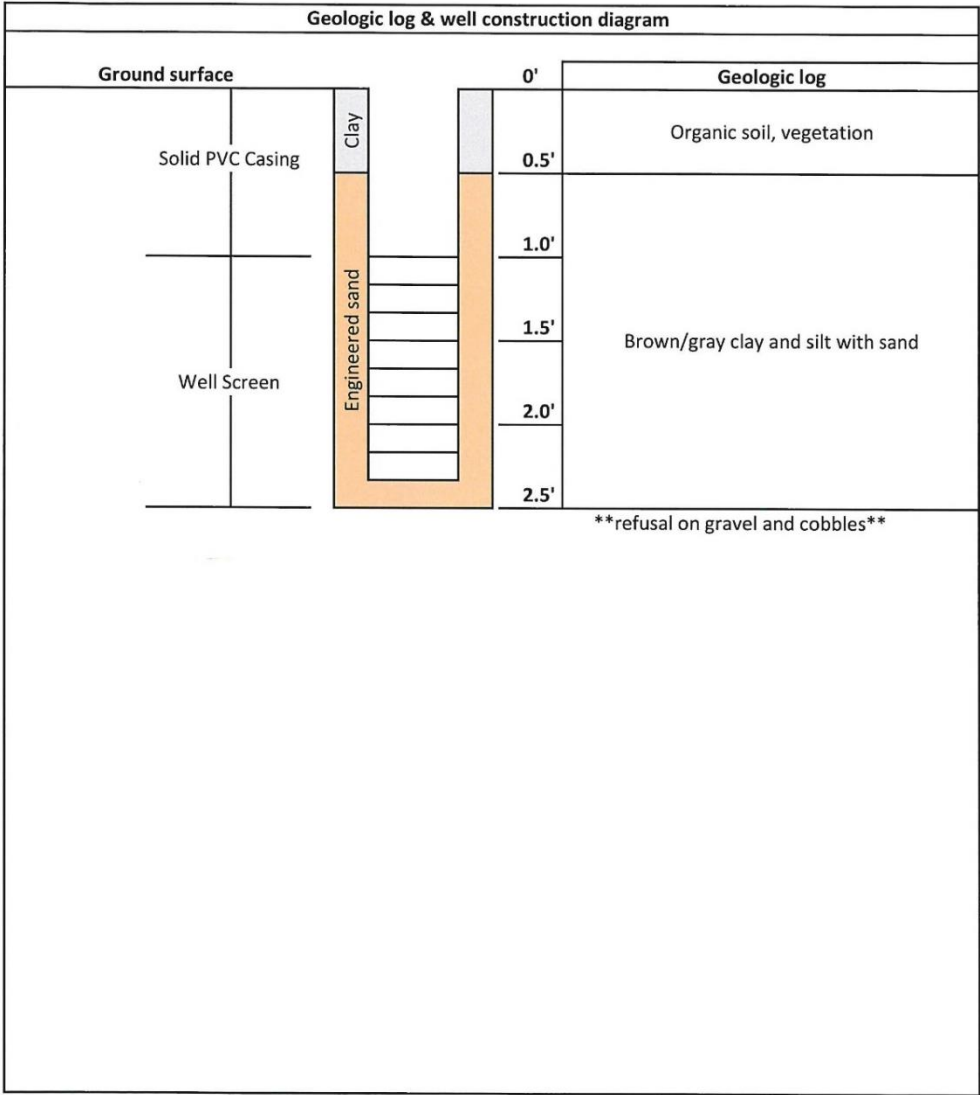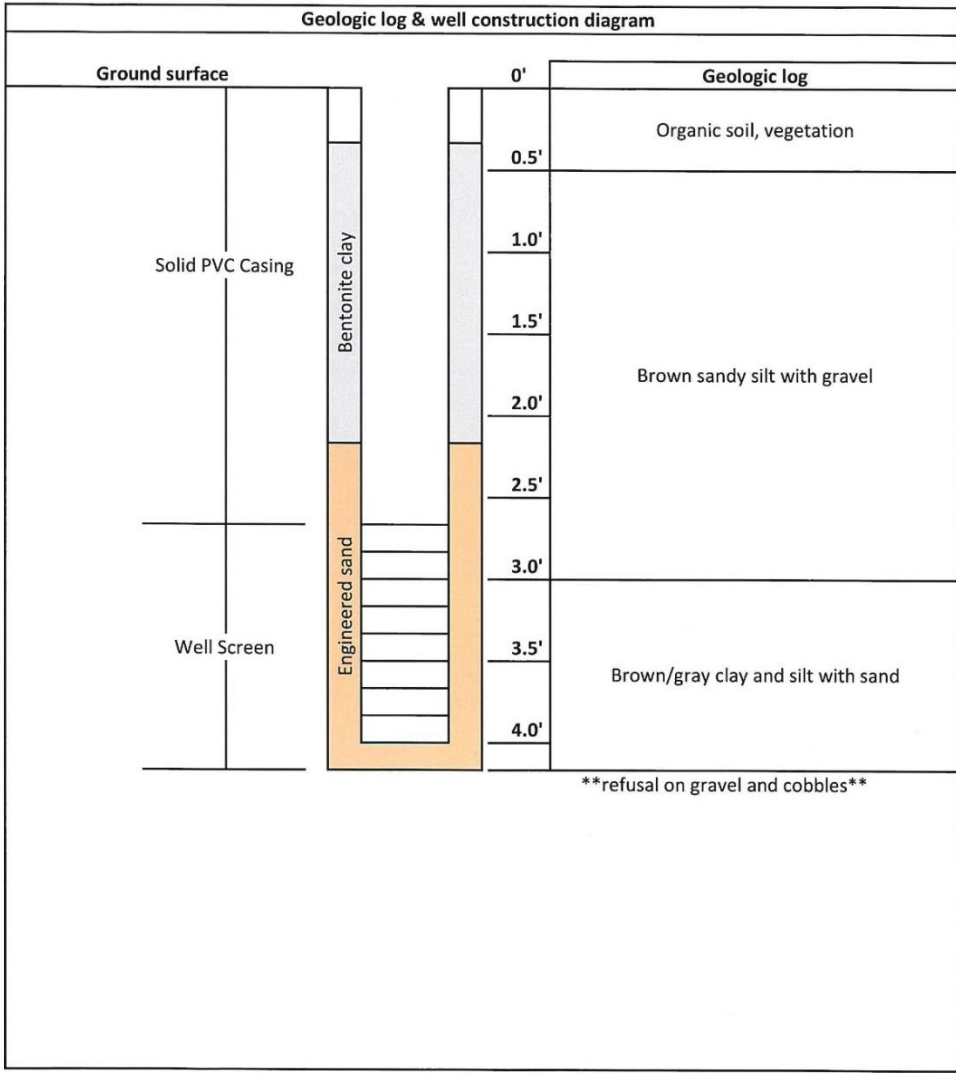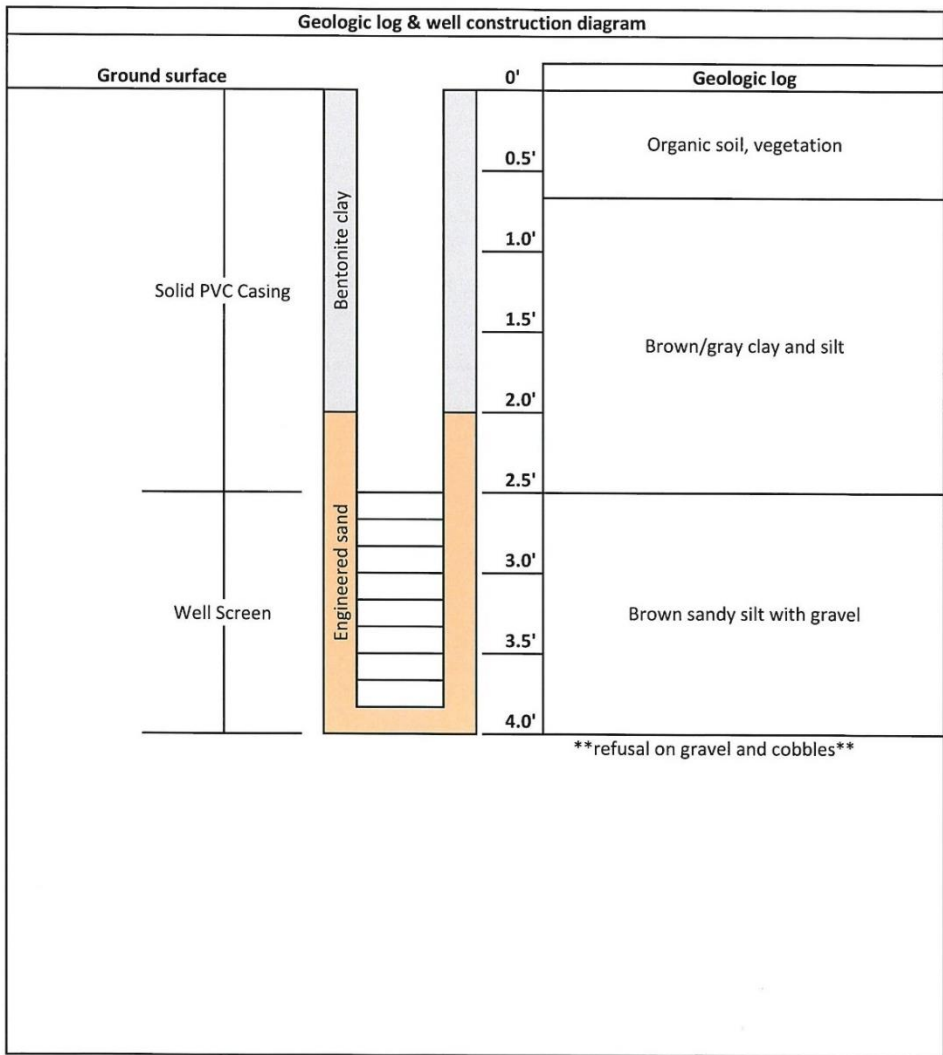Depth markers: 0', 0.5', 1.0', 1.5', 2.0', 2.5', 3.0', 3.5', 4.0'

Appendix B-1-8: Geologic and well construction log for MW8.

| Well ID: | MW9 | Drilled by: | John Lunzer | Date installed: | 6/23/2018 |
| Drilled with: | Hand auger | Logged by: | John Lunzer | PVC diameter: | 1.0 inch |

Appendix B-1-9: Geologic and well construction log for MW9.

Appendix B-2: Hand measured water elevations for the entire monitoring period.

Equipment ID	Water elevations (ft)											
	5/10	5/26 AM	5/26 PM	6/16	6/17	6/22	6/23	7/9	7/14	7/21	8/10	10/13
MW1	3381.69	3382.74	3382.71	3381.52	3381.52	3381.46	3381.51	3380.86	3380.64	3379.99	3379.81	----
MW2	3381.35	3382.50	3382.42	3381.39	3381.39	3381.37	3381.42	3380.76	3380.49	3380.00	3379.33	----
MW3	3380.56	3381.85	3382.54	3381.24	3381.24	3381.22	3381.31	3380.52	3380.30	3379.95	3379.33	3379.18
MW4	3381.66	3382.51	3382.44	3381.51	3381.51	3381.47	3381.56	3380.89	3380.56	3379.97	----	----
MW5	3381.47	3382.61	3382.58	3380.97	3380.97	3380.92	3381.07	3380.24	3380.24	----	----	----
MW6	3382.71	3382.56	3382.45	3381.60	3381.60	3381.62	3381.63	3380.91	3380.62	----	----	----
MW7	3381.62	3382.27	3382.46	3381.12	3381.12	3381.19	3381.20	3380.50	3380.32	----	----	----
MW8							3381.09	3381.40	3381.24	3380.81	3379.14	3379.97
MW9							3381.31	3380.43	3379.90	3379.74	3378.61	3379.91
SG1			3381.76	3380.11	3380.11	3380.09	3380.07	3379.86	3379.76	3379.66	----	3379.56
SG2			3381.91	3380.71	3380.71	3380.76	3380.76	3380.46	3380.26	3379.96	----	3379.01
SG3			3381.62	----	----	----	----	----	----	----	----	----
SG4			3382.44	3381.59	3381.59	3381.59	3381.59	3381.09	3380.69	3380.14	----	----
SG5			3382.28	3381.18	3381.18	3381.23	3381.23	3380.68	3380.48	3380.08	----	----
SG6			3381.82	3379.62	3379.62	3379.62	3379.59	3379.42	3379.32	3379.32	----	----
SG7			3382.41	3381.61	3381.61	3381.61	3381.61	3381.11	3381.01	3380.61	----	----
SG8			3382.35	3381.57	3381.57	3381.60	3381.60	3381.05	3380.75	3380.25	----	----
SG9							3380.05	3380.05	3379.85	3379.80	3379.60	3379.05	3379.35
SG10							3381.43	3381.43	3380.83	3380.63	3380.33	----	----
SG11							3381.57	3381.57	3381.07	3380.92	3380.57	3378.92	3378.90
SG12							3379.53	3379.53	3378.93	3378.63	3378.13	----	3378.20

*dashes indicate dry conditions, blanks indicate data not collected for particular date

Appendix B-3-1: Transducer measured water elevations (July 2018).

Date	Water elevations (ft)								
	MW1	MW2	MW3	MW5	MW6	MW7	MW8	MW9	SG9
7/15/18	3380.32	3380.13	3380.23	3380.22	3380.48	3380.32	3381.22	3379.84	----
7/16/18	3380.27	3380.08	3380.19	3380.18	3380.40	3380.32	3381.18	3379.78	----
7/17/18	3380.22	3380.00	3380.14	3380.13	3380.53	3380.31	3381.08	3379.70	----
7/18/18	3380.17	3379.93	3380.10	3380.10	3380.49	3380.32	3381.01	3379.62	----
7/19/18	3380.12	3379.83	3380.06	3380.06	3380.65	3380.32	3380.90	3379.52	----
7/20/18	3380.06	3379.77	3380.02	3380.02	3380.31	3380.32	3380.86	3379.47	----
7/21/18	3379.85	3379.78	3380.02	3380.01	3380.67	3380.22	3381.01	3379.49	----
7/22/18	3379.74	3379.72	3379.97	3379.96	3380.47	----	3381.01	3379.47	----
7/23/18	3379.68	3379.66	3379.92	3379.90	3380.36	----	3380.91	3379.43	----
7/24/18	3379.63	3379.60	3379.87	3379.86	3380.75	----	3380.82	3379.40	----
7/25/18	3379.59	3379.56	3379.84	3379.82	3380.71	----	3380.76	3379.35	----
7/26/18	----	3379.51	3379.79	----	3380.47	----	3380.51	3379.28	----
7/27/18	----	3379.46	3379.75	----	3380.11	----	3380.52	3379.19	----
7/28/18	----	3379.42	3379.71	----	3380.47	----	3380.51	3379.16	----
7/29/18	----	3379.38	3379.67	----	3380.28	3380.17	3380.50	3379.13	----
7/30/18	----	3379.33	3379.64	----	3380.46	3380.17	3380.46	3379.11	----
7/31/18	----	3379.29	3379.61	3379.70	3380.72	3380.16	3380.27	3379.06	----

*dashes indicate dry conditions, 15-minute water elevation data available upon request

Appendix B-3-2: Transducer measured water elevations (August 2018).

Date	Water elevations (ft)								
	MW1	MW2	MW3	MW5	MW6	MW7	MW8	MW9	SG9
8/1/18	----	3379.27	3379.59	3379.71	3380.49	3380.18	3380.07	3378.95	----
8/2/18	----	3379.23	3379.57	3379.71	3380.69	3380.18	3379.91	3378.82	----
8/3/18	----	3379.23	3379.55	3379.72	3380.69	3380.18	3379.79	3378.74	----
8/4/18	----	3379.20	3379.52	3379.71	3380.53	3380.17	3379.68	3378.71	----
8/5/18	----	3379.17	3379.50	3379.71	3380.23	3380.18	3379.61	3378.71	----
8/6/18	----	3379.14	3379.47	3379.70	3380.40	3380.17	3379.53	3378.69	----
8/7/18	----	3379.15	3379.44	3379.71	3380.73	3380.17	3379.47	3378.69	----
8/8/18	----	3379.15	3379.41	3379.70	3380.69	3380.17	3379.42	3378.68	----
8/9/18	----	3379.15	3379.39	3379.71	3381.25	3380.17	3379.37	3378.67	----
8/11/18	----	----	3379.40	3379.72	----	----	3379.35	3378.69	3379.05
8/12/18	----	----	3379.40	3379.73	----	----	3379.32	3378.67	3379.04
8/13/18	----	----	3379.39	3379.73	----	----	3379.28	3378.71	3379.01
8/14/18	----	----	3379.36	3379.73	----	----	3379.26	3378.76	3378.99
8/15/18	----	----	3379.33	3379.73	----	----	3379.24	3378.79	3378.97
8/16/18	----	----	3379.31	3379.71	----	----	3379.22	3378.82	3378.93
8/17/18	----	----	3379.32	3379.71	----	----	3379.22	3378.85	3378.92
8/18/18	----	----	3379.36	3379.73	----	----	3379.22	3378.86	3378.93
8/19/18	----	----	3379.33	3379.73	----	----	3379.18	3378.81	3378.91
8/20/18	----	----	3379.34	3379.70	----	----	3379.14	3378.77	3378.87
8/21/18	----	----	3379.34	3379.73	----	----	3379.16	3378.83	3378.88
8/22/18	----	----	3379.37	3379.73	----	----	3379.18	3378.87	3378.88
8/23/18	----	----	3379.39	3379.73	----	----	3379.19	3378.89	3378.86
8/24/18	----	----	3379.38	3379.73	----	----	3379.20	3378.91	3378.85
8/25/18	----	----	3379.40	3379.74	----	----	3379.20	3378.91	3378.86
8/26/18	----	----	3379.38	3379.72	----	----	3379.20	3378.94	3378.84
8/27/18	----	----	3379.38	3379.72	----	----	3379.26	3379.03	3378.84
8/28/18	----	----	3379.40	3379.74	----	----	3379.39	3379.22	3378.91
8/29/18	----	----	3379.39	3379.73	----	----	3379.45	3379.22	3378.90
8/30/18	----	----	3379.38	3379.73	----	----	3379.44	3379.17	3378.89
8/31/18	----	----	3379.37	3379.72	----	----	3379.40	3379.13	3378.88

*dashes indicate dry conditions, 15-minute water elevation data available upon request

**Appendix B-3-3:** Transducer measured water elevations (September 2018).

Date	Water elevations (ft)								
	MW1	MW2	MW3	MW5	MW6	MW7	MW8	MW9	SG9
9/1/18	----	----	3379.40	3379.74	----	----	3379.39	3379.13	3378.89
9/2/18	----	----	3379.40	3379.74	----	----	3379.38	3379.13	3378.89
9/3/18	----	----	3379.39	3379.74	----	----	3379.36	3379.11	3378.87
9/4/18	----	----	3379.39	3379.73	----	----	3379.34	3379.09	3378.86
9/5/18	----	----	3379.39	3379.74	----	----	3379.33	3379.08	3378.86
9/6/18	----	----	3379.38	3379.72	----	----	3379.29	3379.04	3378.84
9/7/18	----	----	3379.38	3379.73	----	----	3379.26	3379.01	3378.83
9/8/18	----	----	3379.38	3379.73	----	----	3379.24	3378.98	3378.83
9/9/18	----	----	3379.39	3379.74	----	----	3379.22	3378.97	3378.83
9/10/18	----	----	3379.39	3379.74	----	----	3379.21	3378.99	3378.84
9/11/18	----	----	3379.40	3379.75	----	----	3379.22	3379.02	3378.83
9/12/18	----	----	3379.41	3379.76	----	----	3379.26	3379.08	3378.85
9/13/18	----	----	3379.40	3379.75	----	----	3379.28	3379.11	3378.84
9/14/18	----	----	3379.41	3379.75	----	----	3379.34	3379.19	3378.85
9/15/18	----	----	3379.40	3379.75	----	----	3379.39	3379.23	3378.86
9/16/18	----	----	3379.39	3379.74	----	----	3379.41	3379.25	3378.86
9/17/18	----	----	3379.40	3379.75	----	----	3379.42	3379.23	3378.87
9/18/18	----	----	3379.40	3379.75	----	----	3379.40	3379.21	3378.86
9/19/18	----	----	3379.41	3379.76	----	----	3379.40	3379.21	3378.88
9/20/18	----	----	3379.41	3379.76	----	----	3379.41	3379.22	3378.88
9/21/18	----	----	3379.40	3379.76	----	----	3379.43	3379.24	3378.88
9/22/18	----	----	3379.38	3379.73	----	----	3379.43	3379.24	3378.86
9/23/18	----	----	3379.39	3379.74	----	----	3379.47	3379.29	3378.87
9/24/18	----	----	3379.42	3379.77	----	----	3379.54	3379.35	3378.91
9/25/18	----	----	3379.41	3379.77	----	----	3379.56	3379.32	3378.92
9/26/18	----	----	3379.41	3379.76	----	----	3379.58	3379.35	3378.91
9/27/18	----	----	3379.40	3379.75	----	----	3379.59	3379.35	3378.91
9/28/18	----	----	3379.40	3379.75	----	----	3379.60	3379.36	3378.92
9/29/18	----	----	3379.40	3379.75	----	----	3379.62	3379.39	3378.93
9/30/18	----	----	3379.40	3379.75	----	----	3379.66	3379.44	3378.92

*dashes indicate dry conditions, 15-minute water elevation data available upon request

Appendix B-3-4: Transducer measured water elevations (October 2018).

Date	Water elevations (ft)								
	MW1	MW2	MW3	MW5	MW6	MW7	MW8	MW9	SG9
10/1/18	----	----	3379.41	3379.76	----	----	3379.71	3379.48	3378.94
10/2/18	----	----	3379.38	3379.74	----	----	3379.74	3379.49	3378.93
10/3/18	----	----	3379.37	3379.73	----	----	3379.75	3379.50	3378.92
10/4/18	----	----	3379.39	3379.74	----	----	3379.79	3379.52	3378.95
10/5/18	----	----	3379.42	3379.77	----	----	3379.87	3379.61	3378.99
10/6/18	----	----	3379.40	3379.75	----	----	3379.91	3379.64	3378.99
10/7/18	----	----	3379.39	3379.75	----	----	3380.02	3379.84	3379.04
10/8/18	----	----	3379.41	3379.77	----	----	3380.07	3379.87	3379.08
10/9/18	----	----	3379.38	3379.74	----	----	3380.08	3379.82	3379.09
10/10/18	----	----	3379.39	3379.75	----	----	3380.29	3380.26	3379.30
10/11/18	----	----	3379.42	3379.77	----	----	3380.31	3380.14	3379.35
10/12/18	----	----	3379.42	3379.77	----	----	3380.27	3379.99	3379.36
10/13/18	----	----	3379.42	3379.77	----	----	3380.25	3379.91	3379.36

*dashes indicate dry conditions, 15-minute water elevation data available upon request
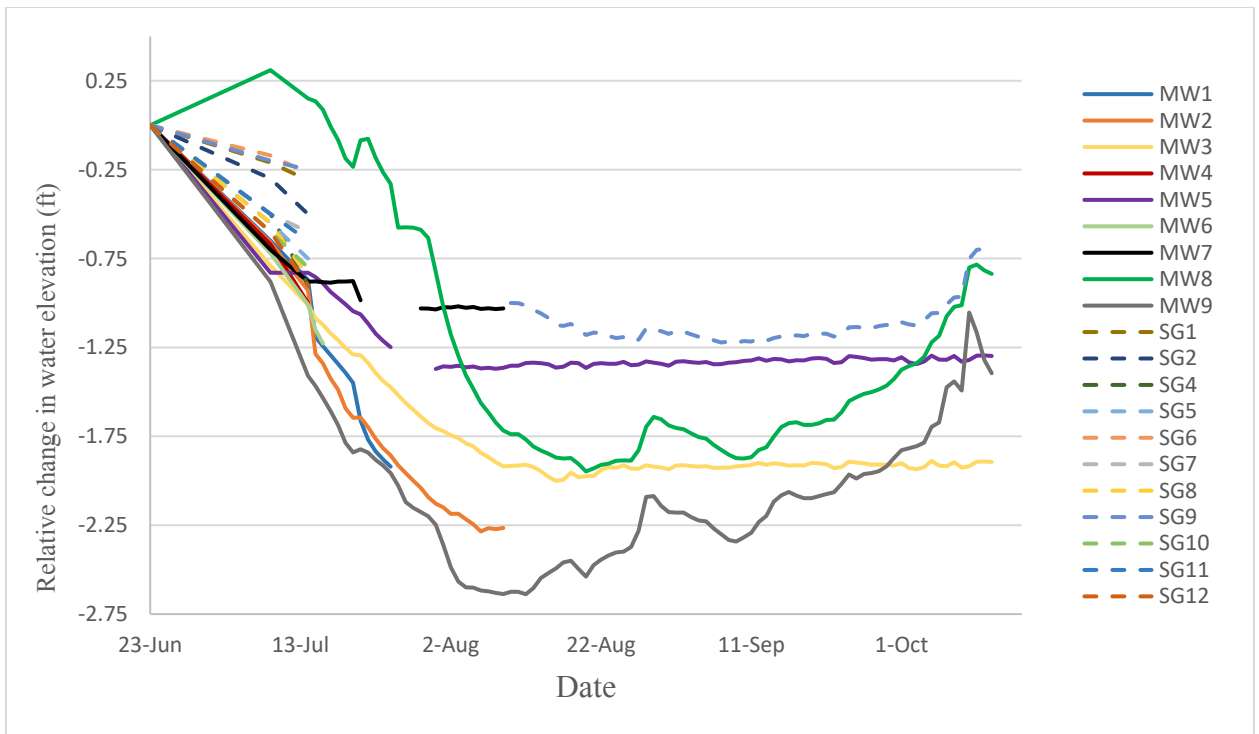
Appendix B-4: Relative change in water elevation for all monitoring equipment over the entire monitoring

period.

Appendix B-5-1: Hand drawn water elevation contours for June 23, 2018.

Appendix B-5-2: Hand drawn water elevation contours for July 9, 2018.

Appendix B-6-1: Temperature measurements in all monitoring equipment measured during site visits.

Equipment ID	Temperature (°C)										
	5/26 AM	5/26 PM	6/16	6/17	6/22	6/23	7/9	7/14	7/21	8/10	10/13
MW1	12.9	12.4	11.8	11.5	12.3	11.9	11.6	12.5	12.2	14.6	----
MW2	12.2	11.6	11.7	11.1	11.7	11.3	11.1	11.9	10.3	12.5	----
MW3	10.8	12.1	11.3	11.3	11.4	11.3	11.2	11.9	12.0	12.0	10.3
MW4	13.6	15.6	13.0	13.0	13.6	14.0	13.1	13.5	13.9	----	----
MW5	12.6	13.9	11.3	11.4	11.6	11.4	11.8	13.5	----	----	----
MW6	15.0	18.5	15.2	14.6	17.0	16.3	16.3	15.6	16.7	----	----
MW7	13.3	13.7	12.6	12.4	12.8	12.6	14.0	14.2	----	----	----
MW8						14.2	14.0	16.2	17.1	14.1	10.0
MW9						14.9	17.3	17.8	18.6	17.7	10.8
SG1		10.2	10.7	10.9	13.3	10.5	11.7	11.5	23.6	----	1.4
SG2		15.2	14.5	13.9	20.2	15.1	15.3	14.8	13.2	----	2.3
SG3		12.3	----	----	----	----	----	----	----	----	----
SG4		16.7	15.5	14.9	21.5	17.2	17.0	19.8	21.0	----	----
SG5		15.0	13.6	14.3	18.7	14.4	15.4	15.7	19.7	----	----
SG6		14.3	16.2	17.4	18.4	14.7	20.2	14.6	25.2	----	----
SG7		14.8	13.1	14.0	19.5	15.5	17.0	16.9	18.3	----	----
SG8		16.1	16.0	16.8	23.9	17.9	18.3	16.8	21.4	----	----
SG9						12.8	12.2	13.3	13.6	13.4	17.5	5.2
SG10						21.8	15.2	13.9	12.7	12.8	----	----
SG11						21.2	16.7	18.4	19.4	23.4	23.3	7.4
SG12						22.2	14.1	17.0	15.9	20.5	----	6.2

*dashes indicate dry conditions, blanks indicate data not collected for particular date

Appendix B-6-2: Specific conductivity measurements in all monitoring equipment measured during site visits.

Equipment ID	Specific conductivity (µS/cm)										
	5/26 AM	5/26 PM	6/16	6/17	6/22	6/23	7/9	7/14	7/21	8/10	10/13
MW1	174	242	189	215	143	172	404	272	413	----	----
MW2	437	439	410	418	415	417	420	434	552	----	----
MW3	490	502	495	495	492	497	488	511	373	507	566
MW4	607	603	643	622	615	638	635	640	979	----	----
MW5	664	549	727	724	747	759	983	1015	1040	----	----
MW6	656	657	688	684	680	689	620	621	1029	----	----
MW7	612	656	642	638	692	722	1035	1054	----	----	----
MW8							268	275	277	284	260	226
MW9							257	280	292	233	522	238
SG1		224	157	168	168	170	161	164	185	----	152
SG2		158	215	214	217	217	247	256	383	----	344
SG3		140	----	----	----	----	----	----	----	----	----
SG4		161	185	186	185	192	215	234	241	----	----
SG5		131	206	210	207	216	236	264	233	----	----
SG6		129	201	219	195	210	219	230	232	----	----
SG7		118	192	195	194	203	214	230	201	----	----
SG8		127	224	225	223	225	255	286	312	----	----
SG9						254	227	242	317	348	463	293
SG10						333	340	381	442	441	----	----
SG11						195	199	210	207	209	211	294
SG12						202	209	220	277	249	----	285

*dashes indicate dry conditions, blanks indicate data not collected for particular date
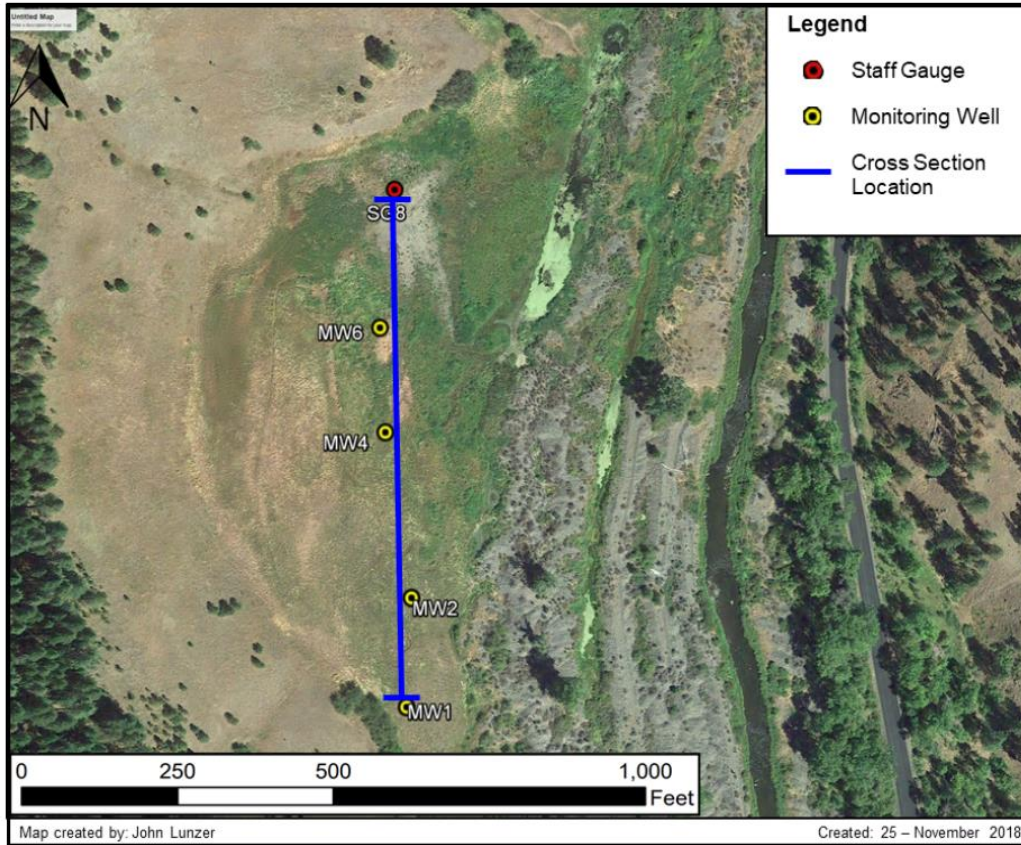
Appendix B-7: Location of the silt/clay layer thickness probing cross section.

Appendix B-8: Raw data from silt/clay layer thickness probing

Distance from MW1 (ft)	Depth to coarse material (in)	Depth to coarse material (ft)
0	12.0	1.0
20	14.0	1.2
40	12.0	1.0
60	2.0	0.2
80	14.0	1.2
100	24.0	2.0
120	24.0	2.0
140	48.0	4.0
160	60.0	5.0
180	22.0	1.8
200	12.0	1.0
220	22.0	1.8
240	48.0	4.0
260	20.0	1.7
280	18.0	1.5
300	54.0	4.5
320	18.0	1.5
340	22.0	1.8
360	14.0	1.2
380	8.0	0.7
400	9.0	0.8
420	6.0	0.5
440	12.0	1.0
460	10.0	0.8
480	18.0	1.5
500	24.0	2.0
520	24.0	2.0
540	30.0	2.5
560	20.0	1.7
580	18.0	1.5
600	24.0	2.0
691	42.0	3.5

Appendix B-10-1: Measured discharge in all Bear Creek channels.

Channel	Discharge (ft³/sec)							
	4/21/2018	5/26/2018	6/16/2018	6/23/2018	7/9/2018	7/14/2018	7/21/2018	10/13/2018
A	1.79	4.61	0.33	0.27	0.26	0.11	0.10	0.13
B	0.47	1.34	0.33	0.29	0.18	0.15	0.12	0.03
C	0.45	1.89	0.00	0.00	0.00	0.00	0.00	0.00
D	0.99	1.66	0.03	0.01	0.00	0.00	0.00	0.00
E	1.28	2.39	0.03	0.00	0.00	0.00	0.00	0.12

Appendix B-10-2: Discharge in the Middle Fork John Day River on the dates Bear Creek was measured.

Date	Discharge (ft³/sec)
4/21/2018	235.0
5/26/2018	363.0
6/16/2018	62.8
6/23/2018	53.9
7/9/2018	28.1
7/14/2018	24.3
7/21/2018	23.2
10/13/2018	25.9

*daily data available from USGS 14043840 gauge station [waterdata.usgs.gov]

11. Appendix C – Data Analysis
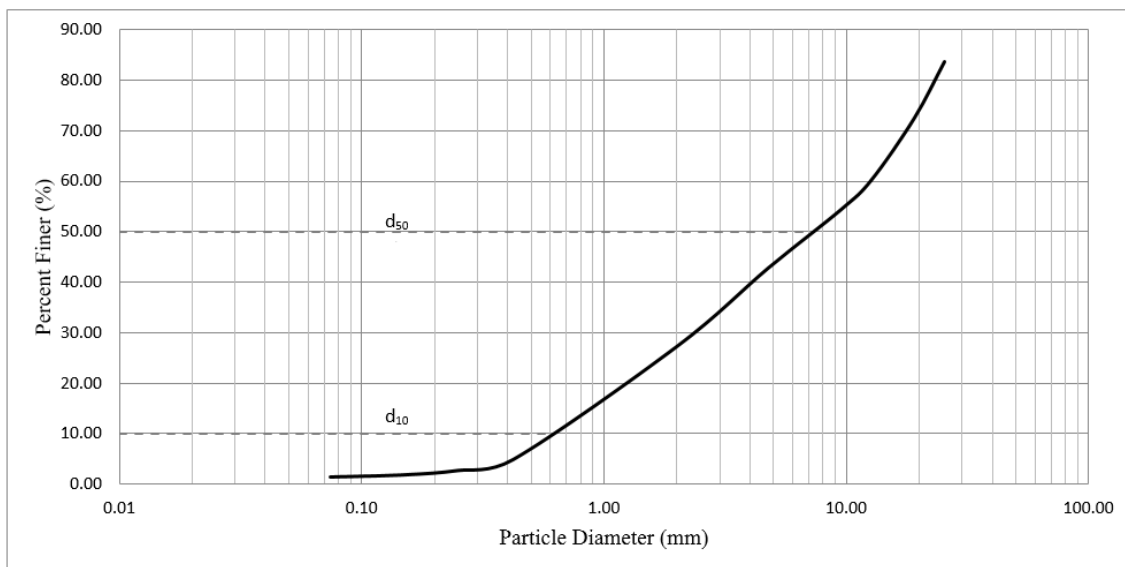
Appendix C-1-1: Particle size distribution curve for Sample #1 taken near MW6.
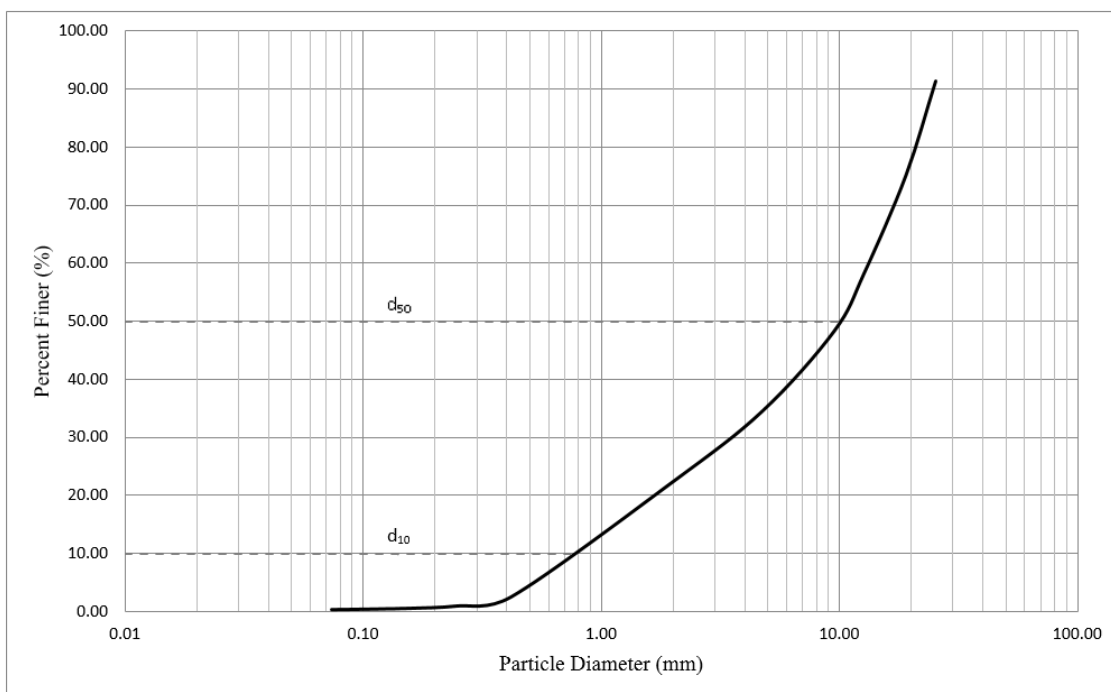
Appendix C-1-2: Particle size distribution curve for Sample #2 taken near MW6.
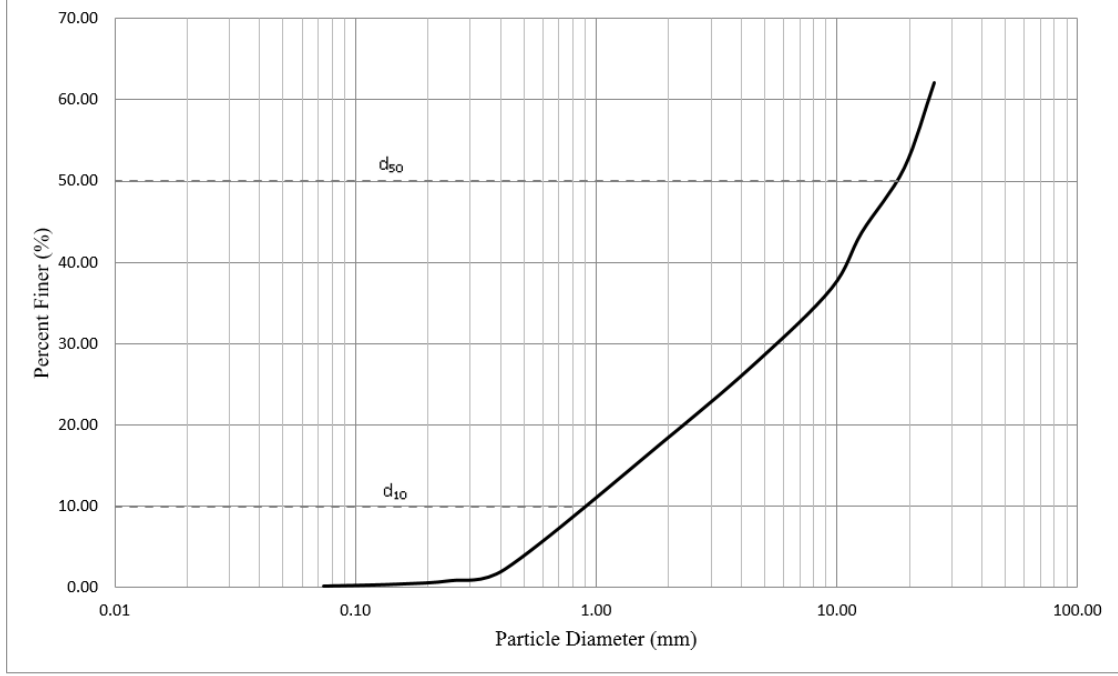
Appendix C-1-3: Particle size distribution curve for Sample #3 taken near MW6.
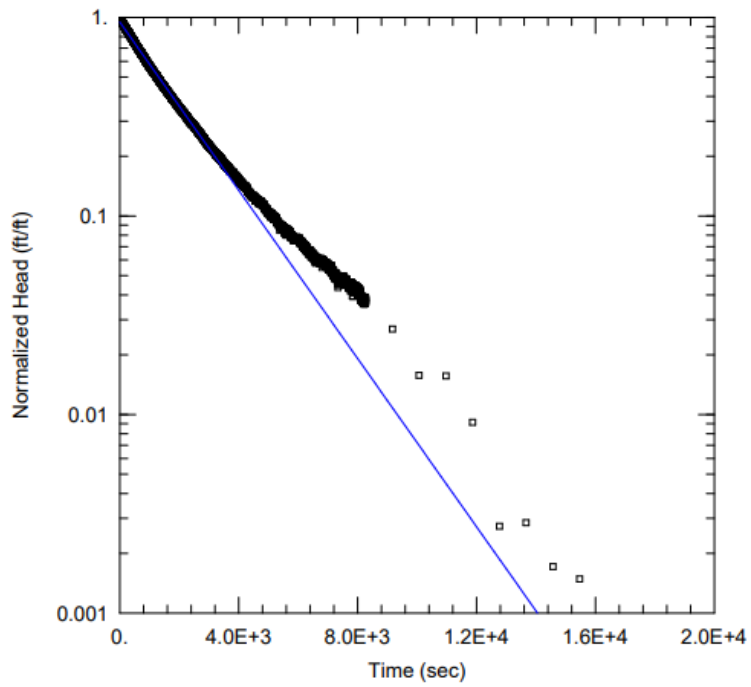
WELL TEST ANALYSIS

Data Set: F:\Galena Tailings Project\Data\07212018_MW3.aqt
Date: 11/23/18   Time: 17:51:40

PROJECT INFORMATION

Project: Galena Tailings
Location: Galena, OR
Test Well: MW3
Test Date: 07/21/2018

AQUIFER DATA

Saturated Thickness: 15. ft   Anisotropy Ratio (Kz/Kr): 1.

WELL DATA (MW3)

Initial Displacement: 0.8764 ft   Static Water Column Height: 1.62 ft
Total Well Penetration Depth: 1.62 ft   Screen Length: 1.5 ft
Casing Radius: 0.04167 ft   Well Radius: 0.0548 ft
                                               Gravel Pack Porosity: 0.3

SOLUTION

Aquifer Model: Unconfined   Solution Method: Hvorslev

K = 0.01771 ft/day   y0 = 0.8292 ft

Appendix C-2-1: Hvorselv analysis – low hydraulic conductivity estimate in MW3 (07/21/2018)

Appendix C-2-2: Hvorselv analysis – high hydraulic conductivity estimate in MW3 (07/21/2018)

Appendix C-2-3: Hvorselv analysis – low hydraulic conductivity estimate in MW8 (07/21/2018)

Appendix C-2-4: Hvorselv analysis – high hydraulic conductivity estimate in MW8 (07/21/2018)

Appendix C-3: GMS – GIS Notes

A variety of data can be imported into GMS from GIS. This includes but is not limited to, observed water levels, top and bottom model elevations and stage level data. When bringing in elevations data from GIS, GMS can read a couple different formats including DEMs and single point data. One should note that GMS will not read multi point data from GIS. Brining these elevations in from raw LiDAR data is a relatively simple process in GIS. The raw las data file must be converted to single point format or DEM/raster format. There are a wide variety of ways to accomplish this task. The one used in this thesis was first converting the raw las data to a LAS Dataset. This LAS Dataset was then converted to a multipoint format file. Once in multipoint format, the file was converted to a single point data file. This single point data file was brought into GMS and used to provide elevations for the top of the model domain. Although this process was relatively simple, newer versions of GMS have powerful built in tools for bringing in raw LiDAR data.

The GMS "Lidar" tutorial describes how to bring raw LiDAR data straight into GMS without using GIS. This tutorial shows how in GMS one can bring in raw las formatted data, process it to the appropriate density and then apply the elevation to either a UGrid or 2D Scatter Data. These built in tools are incredibly powerful and offer the best method for bringing in, processing and applying las data formats into the GMS.
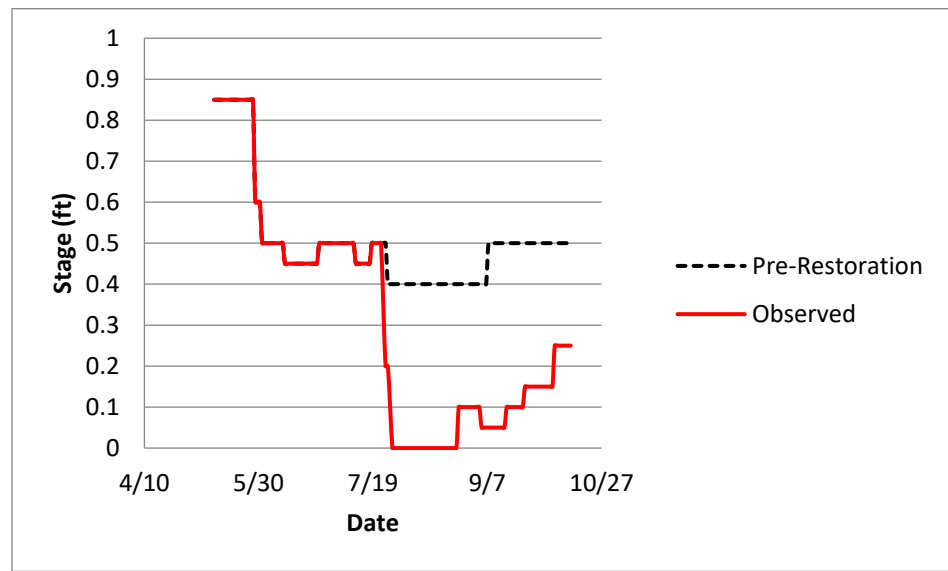
12. Appendix D – Groundwater Model Inputs
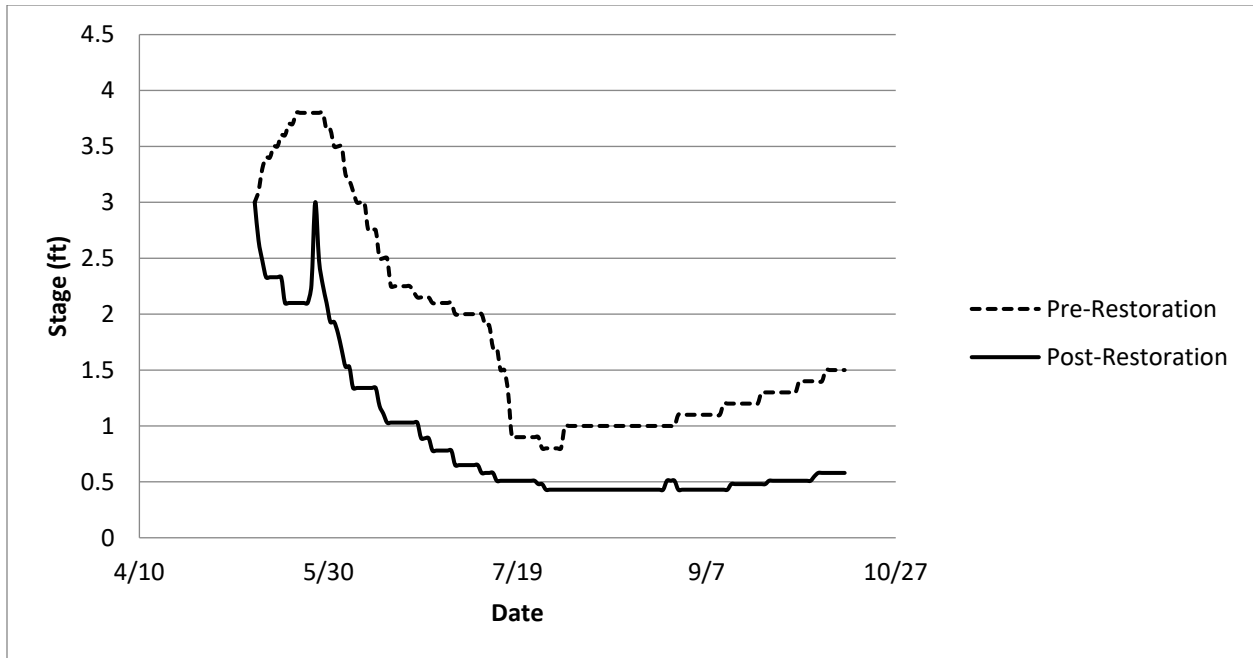
Appendix D-1: Middle Fork John Day River stage level plot input into pre- and post-restoration groundwater models (main channel).
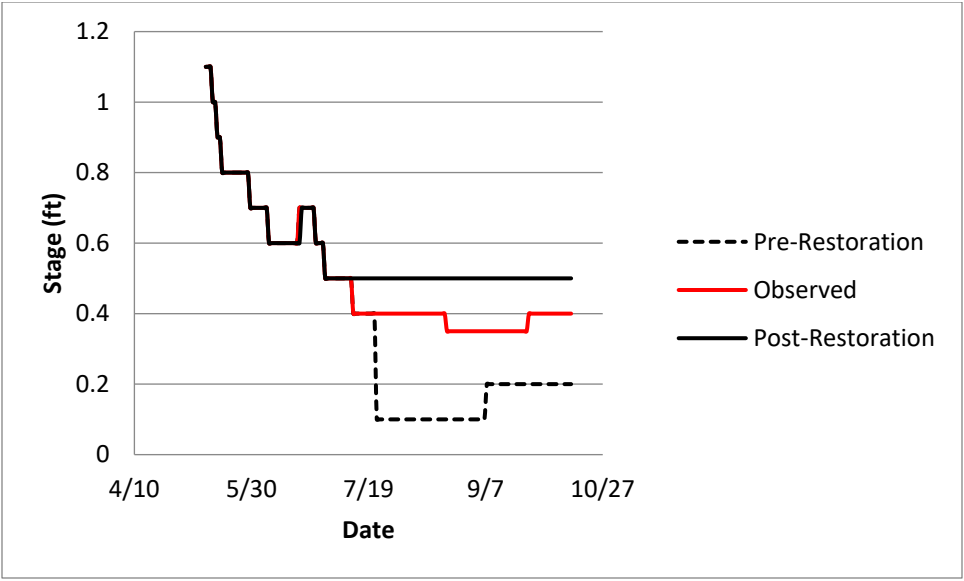
Appendix D-2-1: Bear Creek – Main Channel stage level plot input into pre-, observed and post-

restoration groundwater models (main channel).

Appendix D-2-2: Bear Creek – Channel B stage level plot input into pre-, observed and post-restoration

groundwater models.

SIGNATURE PAGE

This is to certify that the thesis prepared by John Joseph Lunzer entitled "Using Groundwater Modeling to Assess Groundwater and Stream Connectivity in a River Restoration Application" has been examined and approved for acceptance by the Department of Geological Engineering, Montana Technological University, on this 25th day of April, 2019.
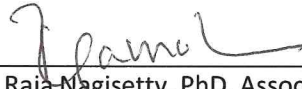
Glenn Shaw, PhD, Professor
Department of Geological Engineering
Chair, Examination Committee
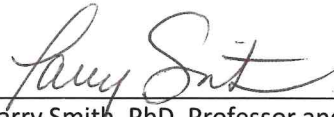
Larry Smith, PhD, Professor and Department Head
Department of Geological Engineering
Member, Examination Committee

Raja Nagisetty, PhD, Associate Professor
Department of Environmental Engineering
Member, Examination Committee

Robert Pal, PhD, Assistant Professor
Department of Biological Sciences
Member, Examination Committee

Liping Jiang, PhD, Assistant Professor
Department of Civil Engineering
Member, Examination Committee